Bulletin of the New Zealand Society for Earthquake Engineering, Vol. 59, No. 3, September 2026

COMPARISON OF SEISMIC RESPONSES USING RECORDED AND SIMULATED GROUND MOTIONS FOR NZS1170.5-BASED 3D STRUCTURAL ANALYSIS

Vahid Loghman[1], Karim Tarbali[2], Brendon A. Bradley[3] and J. Didier Pettinga[4]

(Submitted *July 2025*; Reviewed *September 2025*; Accepted *February 2026*)

ABSTRACT

This paper compares the responses of two 3D building models subjected to recorded and simulated ground motions following New Zealand (NZ) code-based ground-motion selection and scaling provisions to examine the applicability of simulated ground motions for use in conventional engineering practice in NZ. The buildings were designed according to NZ building codes and physically constructed in Christchurch prior to the 2010-2011 Canterbury earthquakes. 40 recorded ground motions from the 22 February 2011 Christchurch earthquake, along with previously published simulated ground motions for this event were considered. The seismic responses of the structures are principally quantified via the peak floor acceleration and peak inter-storey drift ratio. The peak floor accelerations of both buildings, and peak drifts of the 13 storey in-plan regular RC wall structure, were statistically consistent; whereas the peak drifts for the seven storey in-plan irregular mixed system are approximately 30% different. Overall, the results indicate a general agreement in seismic demands obtained using the recorded and simulated ground motion ensembles, and hence provide further evidence that state-of-the-art simulated ground motions can be used in code-based structural performance assessments in place of, or in combination with, ensembles of historically recorded ground motions.

https://doi.org/10.5459/bnzsee.1774

INTRODUCTION

One of the main applications of earthquake-induced ground motion time series (herein GM for brevity) is to conduct dynamic response history analysis for the design and performance assessment of new and existing structures [1,2]. Despite the conventional use of amplitude-scaled GMs recorded from past earthquakes to obtain the response of structures, the most critical issue in their utilisation is the paucity of GMs representing the specific-site hazard conditions, especially for the large magnitude ruptures in the near-fault region. Another restriction is the incompatibility of selected GMs in terms of causal parameters (i.e., faulting style, magnitude, source-to-site distance, basin effects, etc.) with respect to the ruptures affecting the seismic hazard at the site of interest [3].

To overcome these limitations, supplementing recorded GM ensembles with those from simulations is considered a viable option in seismic response analysis of engineered systems if the simulations are of sufficient quality. Ground motion simulation methods have significantly improved in the last decade, enabling engineers to utilise simulated GMs in obtaining seismic responses of engineered systems [4,5]. Although the use of simulated GMs has been accepted by many international design codes [6–8], as well as in New Zealand (NZ) [9], they still do not represent the majority of the use cases in engineering practice due to ambiguity of instructions, insufficiency of detailed validation of simulated GMs, and a general lack of first-hand experience among practitioners in the results compared to those obtained based on recorded GMs. For instance, NZS1170.5:2004 states: *"The ground motion records used for time history analysis shall consist of a family not less than three records. Where three appropriate ground motion records are not available, simulated ground motion records may be used to make up the family."*, which is vague in terms of what constitutes "appropriate" and lacks any specifics on the necessary properties of any adopted simulated GMs.

Validation of simulated GMs is essential to understand the predictive capability of simulation methods, as well as to identify bias and imprecisions that can be utilized by GM simulation modellers to further improve the methods. A 'validation matrix' was proposed by Bradley [1] to encapsulate the many and varied ways in which simulation validation can and should be undertaken. In a NZ-specific context, this includes the comparison of simulated vs. observed ground motions for historical earthquakes of small, moderate, and large magnitudes [10–14] using (simple) conventional intensity measures (IMs). However, the arbitrarily complex 3D seismic response of structures can deviate from that inferred by simple intensity measures, and a comprehensive validation of simulated motions should explicitly assess such structural responses.

Previous international studies have considered validation at different levels of structural response complexity. This includes comparing the responses of nonlinear single-degree-of-freedom (SDOF) systems excited by simulated and recorded GMs [15–18], and the extension to considering 2D multi-degree-

[1] *Structural Engineer, AECOM, Christchurch (Member).*
[2] *Assistant Professor, Université Paris-Saclay, France.*
[3] *Corresponding Author, Professor, University of Canterbury, Christchurch, brendon.bradley@canterbury.ac.nz (Fellow)*
[4] *Holmes Consulting, Christchurch (Member)*

of-freedom systems [4,19–21] for GM simulation validation. However, these studies did not address the response of irregular 3D MDOF systems, including where torsional responses can be a concern, and also did not contextualise their results in the manner in which ground-motion selection and scaling is performed in seismic design codes and standards.

Other studies, such as Burks [22] considered the response of a torsionally-regular 3D MDOF system subjected to a subset of observed GMs, including 11 GMs selected from a global database, and 11 conforming simulated GMs from a specific M_w7.0 earthquake scenario. Also, some efforts have been made in the ground motion simulation context using non-building structures. For example, Galasso et al. [23] compared the responses of skewed reinforced concrete bridges subjected to paired simulated and observed ground motions for two historical earthquakes (i.e., 1989 M_w6.8 Loma Prieta and 1994 M_w6.7 Northridge).

In the context of the above sentiments, this study is focused on comparing the seismic demands of two irregular 3D building models, designed and constructed according to NZ building codes by consulting engineers, when subjected to recorded and simulated GMs from the 22 February 2011 Christchurch earthquake. The seismic response is quantified through commonly adopted engineering demand parameters (EDPs), i.e., peak floor acceleration (PFA) and peak inter-storey drift ratio (IDR). The recorded and simulated GMs are scaled following NZ-specific prescriptions [9,24], and the computed seismic demands are compared. Through analysis and interpretation of the results, it is determined whether the structural responses from simulated GMs are comparable to those from recorded GMs for the considered structural systems, and the opportunity is explored for the use of simulated GMs in engineering design and assessment in the context of NZS1170.5:2004.

The analyses undertaken in this study were completed prior to the draft releases (in 2024) of TS1170.5:2025 [25] and the SESOC nonlinear analysis guidance [24]. As a result, the design spectrum for amplitude scaling the ground motions is that from NZS1170.5:2004. In contrast, and as subsequently discussed, we departed from the NZS1170.5:2004 procedures for ground-motion selection and modification because of their long-recognised limitations, and essentially adopted the essence of the SESOC 2025 guidance.

BUILDINGS PROPERTIES AND MODELLING

Two buildings, a mid-rise and a high-rise, are selected as case studies for nonlinear dynamic analyses. The buildings were originally designed circa 1980 based on NZ standards in their respective eras (NZS4203:1976,NZS3101:1982), and can be considered as examples of existing buildings in Christchurch, and major urban centres in NZ more broadly. 3D views and plans of the selected structures are presented in Figure 1.

The mid-rise building, denoted as Building A, is a seven-storey reinforced concrete (RC) structure with moment-resisting frames in both directions, a boundary wall system in the North-South direction, and shear walls in the East-West direction (see Figure 1a,c). As a result, this structural does exhibit appreciable in-plan torsionality irregularity, as examined later. Also, a lightweight storey was subsequently added to the roof of this building after initial construction. The typical storey height is 3m, except for the first storey and the lightweight storey which are 3.7m and 4.3m, respectively.

The high-rise building, denoted as Building B, consists of a 13-storey tower and a 3-storey podium with a basement. The tower has a hexagonal form in plan, and is separated via a seismic gap from the podium. The tower is a 13-storey structure with ductile RC walls in the East-West direction and ductile RC coupled walls in the North-South direction (see Figure 1b-d). Precast concrete elements were designed for the perimeter truss beams and hollow-core units were used for floors [28]. The typical storey height is 4m for the first two storeys and 3.2m for the other storeys. The podium is not included in the model, and thus the tower response is considered for comparison in this study.

The 3D numerical analysis models of the structures were developed by Holmes Consulting Engineers, using their in-house software which is an extension of the finite element software ANSR [29]. The models use a lumped plasticity approach for modelling nonlinearity. For the beams and columns, a bilinear strain hardening yield function with degradation is used [30]. Coupling beam elements are modelled using equivalent reinforcing content to capture their capacity and backbone curves derived from FEMA 356 coupling beam with diagonal reinforcement [30]. Shear walls are modelled using the FEMA 356 “concrete shear wall segment” definitions [30]. Since concrete wall elements can be controlled by shear or flexural behaviour, appropriate models are used to consider both such behaviours. The shear stiffness of the concrete shear wall elements are modelled using plane stress elements. The modelled behaviour includes strength and stiffness degradation. Table 1 shows the general nonlinear properties of concrete elements according to FEMA356[30] that were used.

A design ductility of 6 was assumed as being the likely value utilised in the design of the buildings, based on the typical approach to ductile seismic design at the time and the level of detailing in the elements. Diaphragms are stiff compared to the vertical elements of the lateral load-resisting system and are therefore modelled as rigid in the analysis. Damping is based on a Rayleigh damping model (5% assigned to the vibration periods equal to 1.5 times the first mode and 90% mass participation mode) using an initial stiffness formulation. Uncertainties in the structural modelling parameters (including accidental eccentricity) were not considered. The fundamental periods for Buildings A and B are 0.5 sec and 2.0 sec, respectively. The 3D nonlinear response history analysis was performed by Holmes Consulting Engineers.

All of the aforementioned modelling assumptions and decisions attempted to emulate those of typical engineering practice in NZ rather than that which may be undertaken in academic research, toward the research objective of a code-based assessment of the use of recorded and simulated ground motions.

OBSERVED AND SIMULATED GROUND MOTIONS

The case study buildings were subjected to bidirectional horizontal ground motions from the 22 February 2011 Christchurch earthquake - both observed and simulated motions. The previously published simulated GMs from Razafindrakoto et al. [31] for this specific event were directly adopted. These simulated ground motions were based on a so-called hybrid broadband method [32,33] in which a comprehensive physics-based approach at low-frequencies ($f \leq 1$ Hz, $T \geq 1$ s) is combined with a simplified physics approach at high-frequencies ($f \geq 1$ Hz, $T \leq 1$ s). Records from 40 stations located in the Canterbury region on a range of different soil conditions ($155 < V_{s30} < 800$ m/s) were considered. Detailed information about the station locations and their V_{s30} values are available in the Appendix. It is noted that three of the considered sites (CSHS, LPCC, MQZ) are located on stiff soil/rock conditions that are not site class D. Records from these three sites, once amplitude scaled to the same target spectra, were not seen to produce any systematically

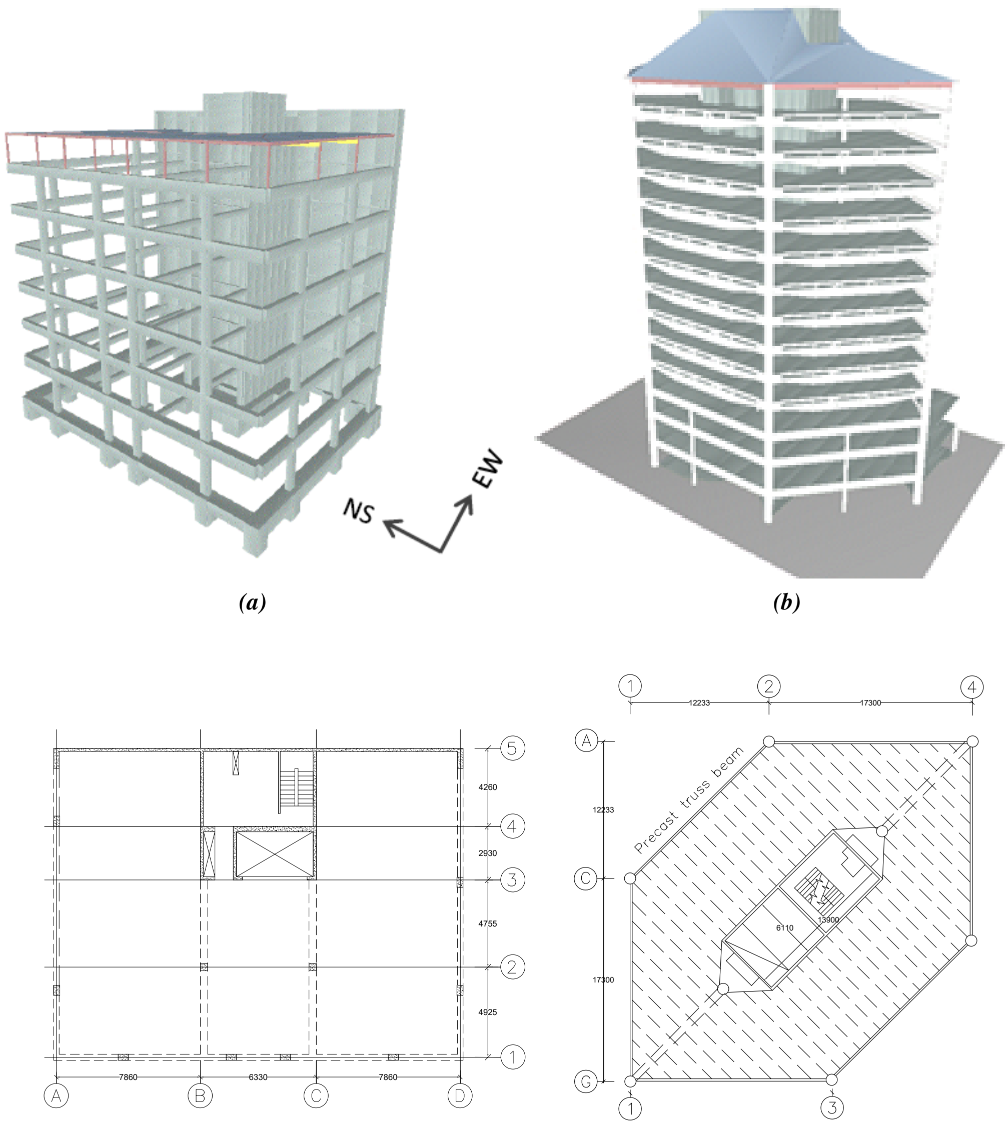

Figure 1: 3D and typical plan views of selected case study structures: (a,c) mid-rise Building A; (b,d) high-rise Building B.

Table 1: Nonlinear Element Parameters based on FEMA356 [30] adopted in the practice-oriented ANSR analysis models.

Nonlinear Parameters FEMA	a	b	c	Generalised Force-Deformation Relations
MRF beams with conforming transverse reinforcement	0.025	0.05	0.2	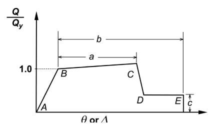
MRF columns with conforming transverse reinforcement	0.02	0.03	0.2	
Coupling beams with diagonal reinforcement	0.03	0.05	0.8	
	d	**e**	**c**	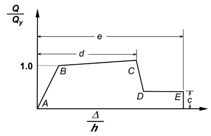
Shear wall and shear wall segments	0.0075	0.02	0.4	

different seismic responses; hence they were retained in order to consider all results from the Razafindrakoto et al. simulations of this event.

Figure 2 illustrates the geometric mean of the 5% damped (pseudo) spectral acceleration of the observed and simulated GMs at the 40 stations considered; indicating that the GMs span a wide range of intensity as a result of variation in the source-to-site distance and soil conditions, among other factors. Herein, the geometric mean of the two horizontal components is considered the representative GM metric for each station, consistent with the ongoing practice in NZ.

Consistent with the 'ordinary office building' nature of these two case study structures, they are classified as Importance Level 2 with a 50 year design service life as per NZS1170.5:2004. As a result, the 475-year return period was used as the ULS design level, and hence the response spectrum for this return period (for site class D soil conditions) was used as the target spectrum for ground motion scaling for both the simulated and observed ground motion sets. Following prescriptions in NZS1170.5:2004, the scaling was performed such that the differences with the target spectra are minimised for the 0.4T_1 - 1.3T_1 range (T_1 being the fundamental period of the structure). The same scaling factor obtained is applied to both components. Then, the scaled ground motion components are applied simultaneously in the principal directions to the structures. The "000" component of the ground motion was applied in the North-South direction and the "090" component in the East-West direction. The effects of the vertical component of GMs are not considered in the analysis, as would be typically the case for such structures in practice.

NZS1170.5:2004 was originally developed in 2004, and the code provisions for response history analysis have undergone many advancements in recent years. As a result, NZ practitioners tend to consider more updated codes such as [7] or a mixture of NZS1170.5:2004 and ASCE 7 for performing response history analysis. Toward the objective to follow conventional NZ practice we made some deviations from the NZS1170.5:2004 provisions in the details of selecting and scaling GMs (it is noted that this study was commenced prior to the recently published SESOC guidelines that include guidance on ground-motion selection for nonlinear response history analysis [24], but our approach is consistent with these guidelines). Specifically, we considered structural response metrics based on 11 GMs from the ensemble of 40 available GMs; each ground motion was amplitude-scaled to minimise the misfit to the target spectrum based on the geometric mean of the two horizontal components; no further modifications to the scale factors of the ensemble of ground motions was applied (i.e., no k2 'family factor' from NZS1170.5:2004, or directional bias check from the 2025 SESOC guidelines).

Figures 3a-d show the scaled observed and simulated GMs in the considered period range for Building A and B, and Figures 3e-f compare the median of the scaled GM ensembles with respect to the NZS1170.5:2004 response spectrum. Given the fundamental vibration periods of the two structures, it can be loosely stated that the peak drift response of building B ($T_1 = 2.0s$) is dominated by the comprehensive physics component of the simulations ($f < 1Hz$), and the peak floor accelerations of both buildings, is dominated by the simplified physics component ($f > 1Hz$). The peak drift response of building A ($T_1 = 0.5s$), is close enough to the $f < 1Hz$ transition frequency that nonlinear response that causes an elongation in the effective secant first mode could be affected by a combination of the comprehensive and simplified physics components of the simulations.

While the scaling produces similar medians for both observed and simulated ensembles, it is noted that the median of the observed GM ensembles is greater than the simulated ensemble for vibration periods larger than the scaling range for Building A (1.3T_1<T<1.4 s), which has implications for the analysis results discussed subsequently when nonlinearity results in the Building A response being sensitive to vibration periods larger than $1.3T_1$.

COMPARISON OF ENGINEERING DEMAND PARAMETERS

Considered Engineering Demand Parameters (EDPs)

The PFA and peak IDR at each floor and across all floors are selected as the principal EDPs, as they are appropriate representatives of damage in non-structural and structural components, and commonly used by building codes [e.g., 7] to satisfy the defined design criteria. Other responses such as displacement and base shear are presented in the Appendix. The considered EDPs are reasonably represented as lognormally distributed [34,35] and their geometric mean, 16^{th}, and 84^{th} percentiles are subsequently presented to compare responses. In order to investigate the effects of torsion, the ratio of maximum corner displacements to the displacement at the centre of mass is calculated and compared along the height of the structures [36–38] for simulations and observations. Since the results in the two principal directions (i.e., North-South and East-West), are found similar in terms of the final outcomes, responses in the North-South direction are mainly discussed in the text. The results in the East-West direction are available in the Appendix.

Comparison Between the EDPs for the Scaled Ground Motions

Figure 4 shows the geometric mean, the 16^{th}, and 84^{th} percentiles of simulated and observed EDPs for the 40 GMs at each floor centre of mass along the height of buildings. Figure 4a shows a small difference between the observed and simulated PFA for Building A. The ratio between the geometric mean of simulated and observed values for the storey with the maximum difference (the sixth storey) is 0.89. As shown in Figure 4b, the simulated GMs underestimate the IDR for Building A. The IDR for the simulated GMs is about 0.77 of the corresponding observed GM value (calculated at the first storey), and this remains relatively constant along the height of the building. It is worth mentioning that although the simulated GMs tend to underpredict the IDR, the response profile over the height is the same for both the simulated and observed GMs. As shown in Figures 4a-b, the 16^{th} to 84^{th} percentile range is smaller for PFA than that for IDR.

Since the paired simulated and observed GMs are amplitude-scaled to the NZS1170.5:2004 response spectrum in a specific period range, the underestimation in IDR by simulations can potentially be attributed to the greater median value of the observed GM spectrum beyond the period range used in the GM scaling (as annotated in Figure 3e), i.e., that the nonlinear structure has sensitivity to the ground motion at vibration periods beyond that (linear elastic) fundamental period, for which the median of observed GMs is larger than those of the simulations. It is worthwhile to mention that NZS1170.5:2004 has the narrowest scaling range (0.4T_1 - 1.3T_1) in comparison to the other building codes such as [7], and [8], where their proposed scaling method covers a broader period range (0.2T_1 - 2T_1) that may affect the response of structures. It is probable that when the structure experiences a high nonlinear level of response, the limited NZS1170.5:2004 scaling range is not sufficient to cover the vibration period range that the inelastic structure is sensitive to.

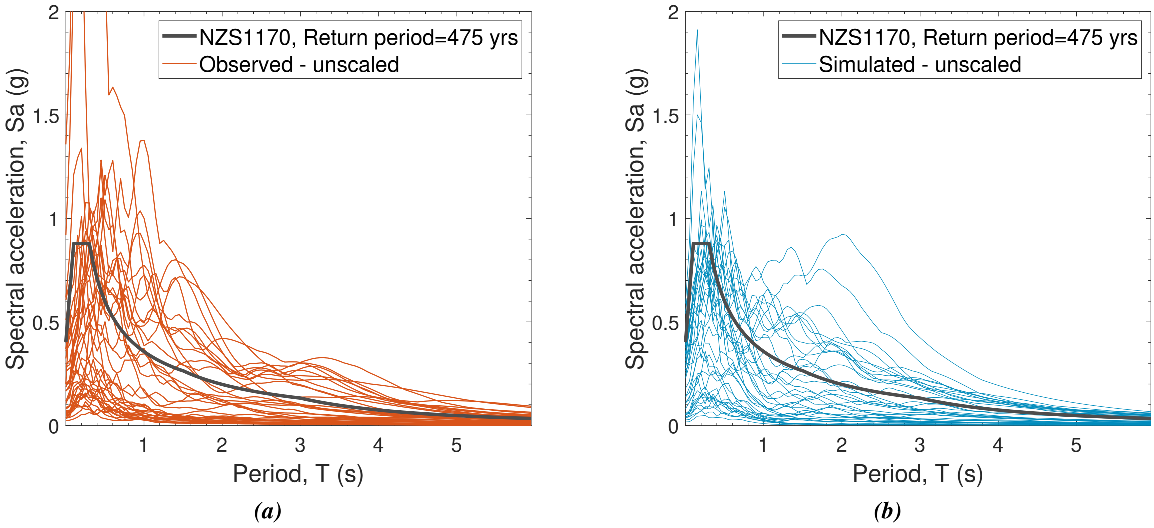

Figure 2: Geometric mean response spectra for the 40 unscaled GMs: (a) observed; and (b) simulated from 22 February 2011 Christchurch Earthquake.

Figures 4c-d present a good agreement between the EDPs of simulated and observed responses along the height of the structure for Building B. The ratio between the geometric mean of simulated and observed values for the storey with the maximum difference is 0.93 for PFA (the 12^{th} storey) and 1.06 for IDR (the sixth storey), which is almost constant along the height of the building for both EDPs. In contrast to Building A, the uncertainty range between the 16^{th} to 84^{th} percentiles for PFA is comparable for the observed and simulated dataset. The absolute value of all responses is available in the Appendix.

The difference between the mean EDP based on the observed and simulated ground-motion sets (approximately 10% from Figures 4a,c, and d) should be considered in the context of typical levels of variability in the distributions of EDP given IM. That is, record-to-record variability and other sources of epistemic uncertainty typically each have lognormal standard deviations of 0.4 [39–41], giving a total apparent aleatory and epistemic uncertainty standard deviation of 0.56. Thus, this 10% difference in the mean seismic response is small compared with a distribution that typically has a lognormal standard deviation of 0.56.

In order to investigate torsional responses, the maximum corner displacement is normalised to the centre of mass displacement at each storey. This ratio is calculated for each set of simulated and observed GMs separately, and then the geometric mean and percentiles are shown in Figures 5a-d for each building and direction. For Building A in the North-South direction (Figure 5a), and Building B in both directions (Figures 5c-d), there is no appreciable difference between simulated responses with respect to the observed ones. In contrast, Figure 5b illustrates an underestimation in the geometric mean of torsional responses by simulated GMs in the East-West direction for Building A, (with a ratio of 0.9) which is almost constant along the height of the structure.

Comparing Figure 5b with 5a shows a higher variability in the torsional responses in the East-West direction than in the North-South direction. This indicates that the building experiences a small to a high amount of torsion in the East-West direction when subjected to simulated and observed GMs. This range, which is higher for the observed GMs, likely depends on to what extent the system experiences nonlinearity when subjected to different records in each set and other complexities in the structure. In contrast, the building in the North-South direction always experiences a high amount of torsion in the plan for both sets of records. Figures 5c-d show that there is a good agreement between the torsional responses of simulated and observed GMs for Building B in both directions. It is worth noting that the variability of ratios along the height is almost constant in Building A, while it decreases along the height for Building B.

Figure 6 illustrates the location of maximum response for Buildings A and B. As shown in Figures 6a-b the peak IDR and PFA occur at the seventh storey of the mid-rise Building A. It is expected that the maximum response occurs in the lightweight storey added to the top of the RC frame. The peak IDR is distributed among different storeys for the high-rise building (Building B) due to the contribution of higher modes in the response (Figure 6c). PFA is localised at the roof level (Figure 6d). In all cases, there are no noticeable differences in capturing the location of maximum response between the simulated and observed ground motions.

EFFECT OF GROUND-MOTION INTENSITY ON SEISMIC DEMAND COMPARISON

Comparison of Ground-Motion Intensity Measures (IMs)

As discussed in the previous section, the difference in the simulated and observed responses can be examined by exploring the differences in the IMs of the observed and simulated GMs. This section therefore examines the statistical significance of any differences between various IMs of the observed and simulated ground motion ensembles.

Figures 7 and 8 compare the distribution of simulated and observed GMs in terms of cumulative density function (CDF) for different intensity measures for Buildings A and B. The Kolmogorov-Smirnov (K-S) test is performed to ascertain whether two distributions are statistically distinct [42]. The null hypothesis is that both samples come from the same continuous distribution. The K-S test bounds for the dataset of 40 GMs with a 5% significance level (for observed GMs) are plotted in Figures 7 and 8 and the *p-value* is calculated. As 11 GMs are usually used based on the new code provisions [7,24], the

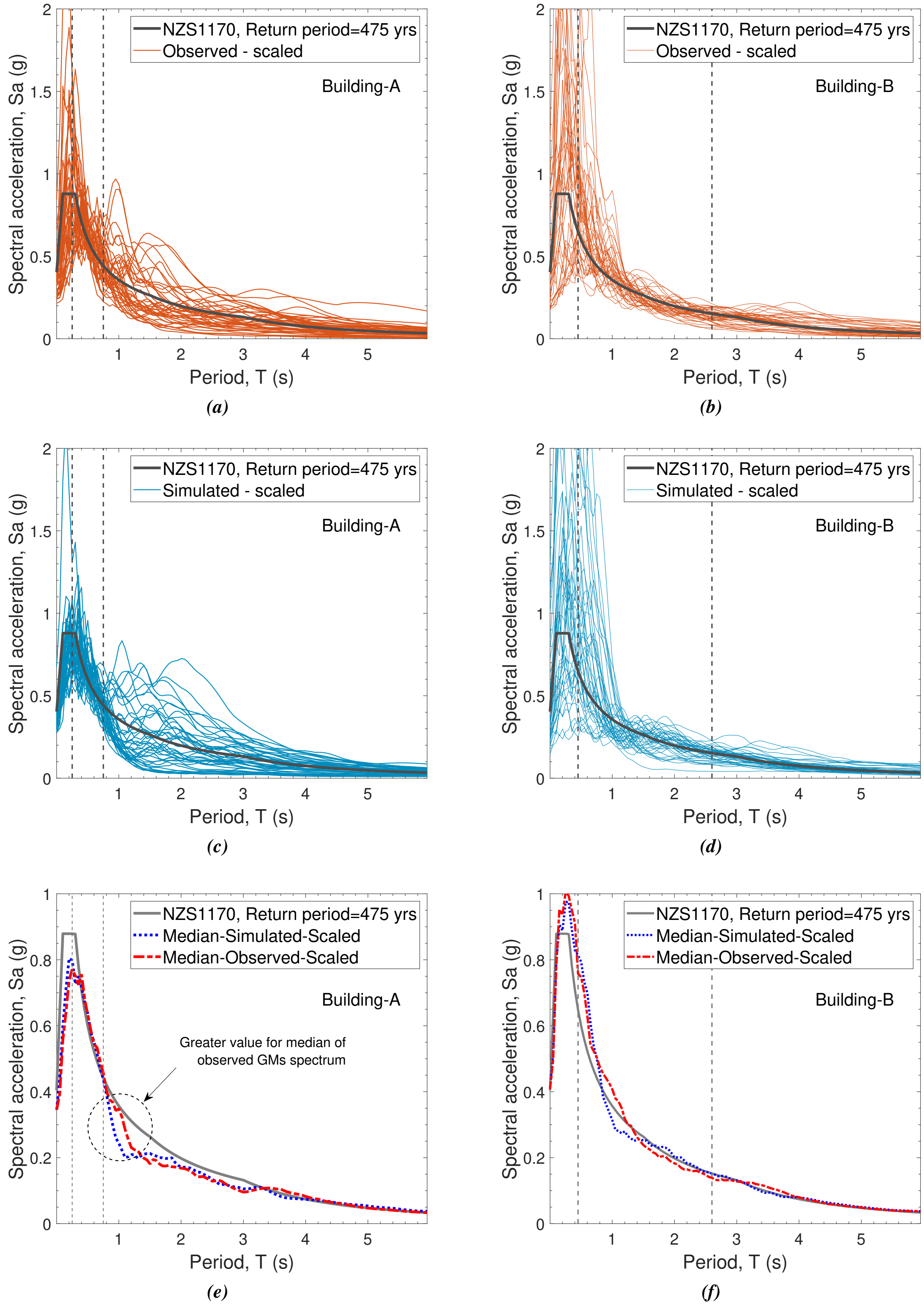

Figure 3: Geometric mean response spectra for the 40 scaled (a-b) observed GM; (c-d) simulated GMs; (e-f) median of observed and simulated GMs; for Building A and Building B. Vertical dashed lines indicate the period range considered for scaling ground motions.

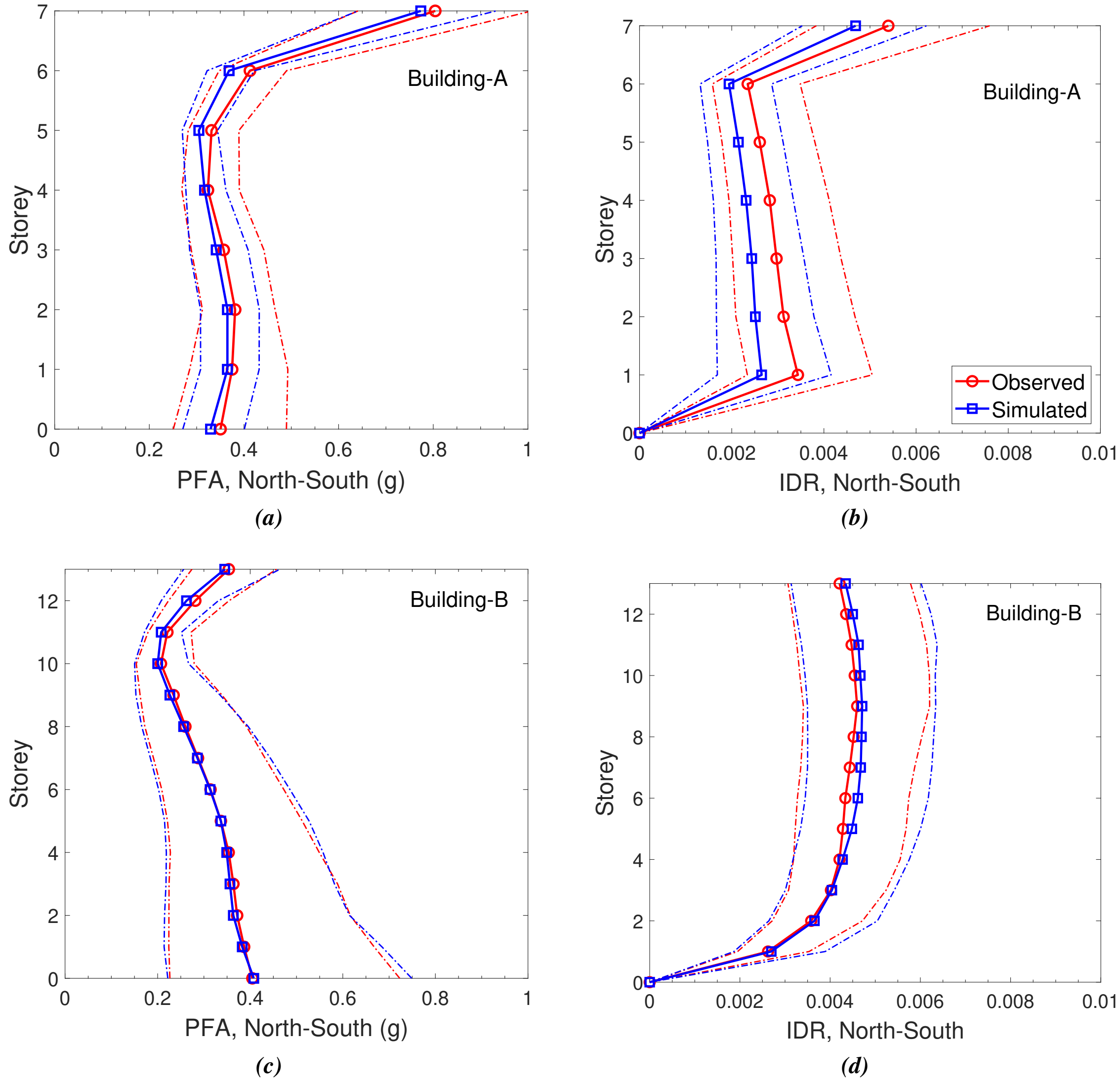

Figure 4: The geometric mean, 16^{th}, and 84^{th} percentiles of simulated and observed responses at the centre of mass for (a) Building A PFA (PFA); (b) Building A inter-storey drift (IDR); (c) Building B PFA; (d) Building B IDR in the North-South direction. Solid lines indicate the geometric mean and dashed lines indicate 16^{th}, and 84^{th} percentiles.

rejection bounds for 11 GMs with a 5% significance level are also shown in the figures. In the K-S test, larger sample sizes can increase the power of the test to detect differences between the two distributions, making it more likely to reject the null hypothesis when there are true differences. Thus, the test bounds for the larger dataset (40 GMs) are narrower than for the smaller dataset using 11 GMs. Visually speaking, if the distribution for simulated GMs lies 'outside' the K-S test bounds for a α =5% significance level (p-value < 0.05), it indicates there is evidence for rejecting the null hypothesis that the simulations and observations are from the same distribution. Figures 7 and 8 illustrate this comparison for Sa(T_1), Sa($2T_1$), PGA, and D_{s595} for Buildings A and B, respectively. Sa($2T_1$) serves as an example of a GM intensity measure beyond the scaling range, where the structural response may be affected in case of experiencing period elongation.

As shown in Figure 7, the difference between the simulated and observed distribution is not statistically significant for Sa(T_1) and PGA, while it is statistically significant for Sa($2T_1$) and D_{s595} for Building A. Figure 8 illustrates a similar comparison between the distribution of simulated and observed GMs for Building B. As shown, only the distribution for D_{s595} is statistically different, while the others are within the K-S test bounds. While the distribution is detected as statistically different for Sa($2T_1$) and D_{s595} for Building A, and D_{s595} for Building B, using a larger dataset (40 GMs), the distribution is within the test bound using 11 GMs (Figures 7b-d, 8d). This implies that using a larger dataset will increase the test power. Given that the distribution of certain GM intensity measures can be statistically different and this may affect the response of interest, the correlation between the intensity measures and the responses is investigated in the following section.

In addition to the discussed intensity measures, the $Sa_{RotD100}/Sa_{RotD50}$ ratio is compared for simulated and observed GM dataset as the measure of polarization. Sa_{RotD50} and $Sa_{RotD100}$ are defined as the median and maximum of spectral acceleration across all orientations, respectively [43,44]. The $Sa_{RotD100}/Sa_{RotD50}$ ratio indicates the degree to which a response of an SDOF is polarized over all orientations subjected to ground motion. The ratio changes between 1 to $\sqrt{2}$ for nonpolarized to highly polarized ground motion [45]. It can be regarded as an indicator of the response of azimuth-dependent systems or torsional-sensitive structures [46]. Figure 9 shows the geometric mean and percentiles for the $Sa_{RotD100}/Sa_{RotD50}$

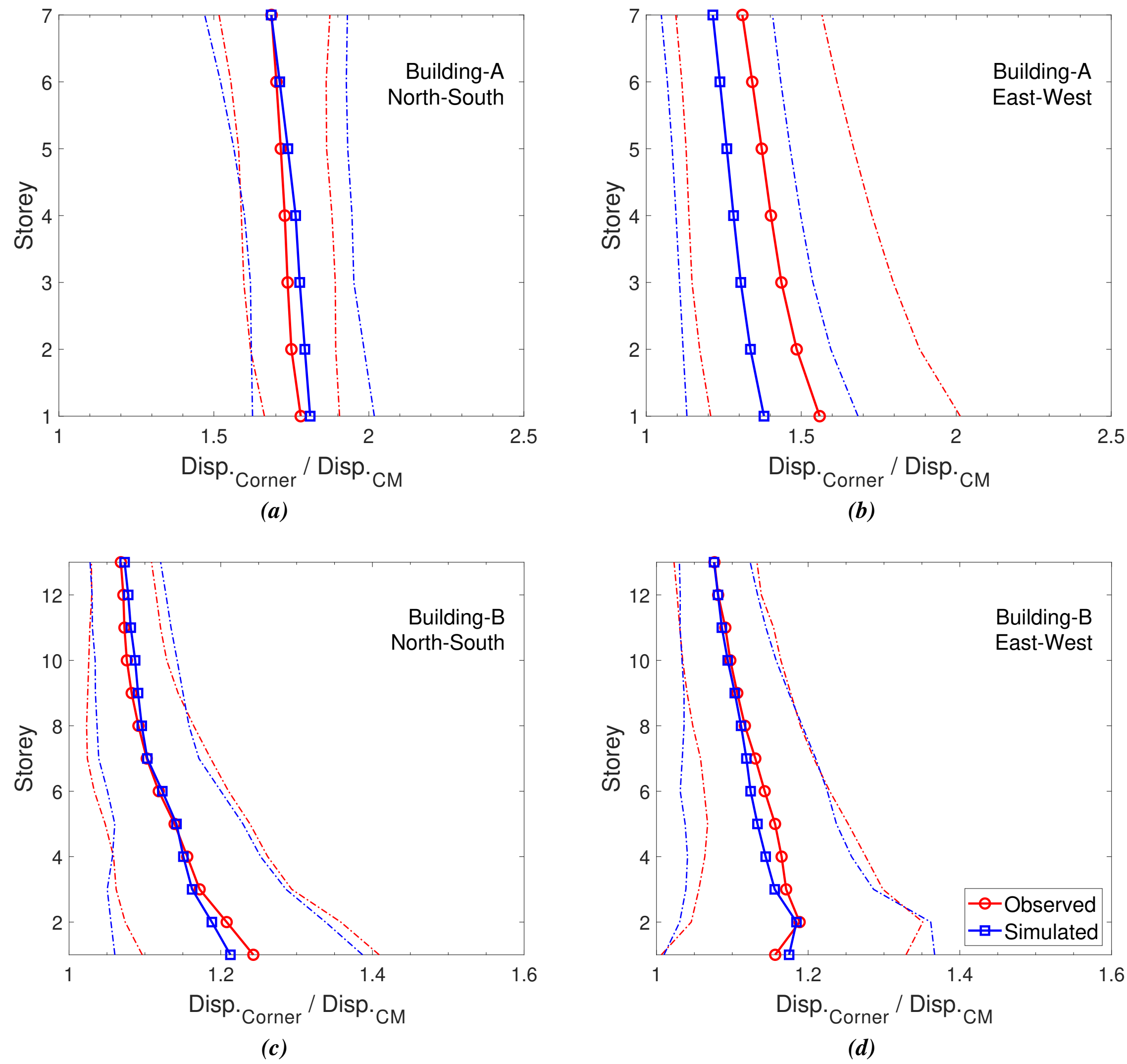

Figure 5: The geometric mean, 16^{th}, and 84^{th} percentiles of the maximum corner to centre of mass displacement for simulated and observed GMs; (a) Building A North-South; (b) Building A East-West; (c) Building B North-South; (d) Building B East-West directions. Solid lines indicate the geometric mean and dashed lines indicate 16^{th}, and 84^{th} percentiles.

components, as well as other non-Sa IMs, for simulated and observed GMs. The fundamental periods of Buildings A and B are also shown in this figure. In general, there is a good agreement between the simulation and observation, specifically, the $Sa_{RotD100}/Sa_{RotD50}$ ratio is quite similar at the fundamental periods of the considered buildings. The only exception is at very short periods (e.g., PGA) where this ratio is higher for the observed ground motions.

Comparison of EDP-IM Relationship

In order to further investigate the variation in EDPs with respect to GM properties, the EDPs are examined as a function of different IMs. IMs with the highest correlation to the responses, calculated based on the Pearson correlation coefficient, ρ, [42], are selected for comparison. The maximum PFA across all storeys (PFA_{max}) is compared with respect to the PGA (Figures 10a and 11a). The peak IDR across all storeys (IDR_{max}) for Buildings A and B is compared with respect to $Sa(2T_1)$ and $Sa(0.5T_1)$, respectively (Figures 10c and 11c). The highest correlation of IDR_{max} with spectral acceleration at periods greater than the fundamental period implies the effects of period elongation due to experiencing nonlinear behaviour in the structural system for Building A, while the highest correlation of IDR_{max} with spectral acceleration at periods smaller than the fundamental period implies the effects of higher vibration modes for Building B.

Figures 10a and 11a demonstrate a good agreement between the observed and simulated PFA_{max} with respect to PGA. As shown in these figures, the simulated and observed EDPs are quite comparable. Figures 10c and 11c illustrate the variation of IDR_{max} versus spectral accelerations at selected periods, showing a similar trend between the simulated and observed EDPs with respect to the considered intensity measures for Buildings A and B. Figures 10(b, d) and 11(b, d) compare the relation of responses with D_{s595}. Although it is shown that the D_{s595} distributions are statistically significantly different for simulations and observations, overall, there is a near-zero correlation between the considered responses and D_{s595}. The EDP-IM comparison of simulated and observed ground motions in the East-West direction is available in the Appendix.

It should be noted that, although the amplitude scaling in the period range specified by NZS1170.5:2004 alleviates differences between simulated and observed GMs to some extent, the misfits between the response spectra of simulations and observations outside the scaling range (Figure 3e) can affect the response in

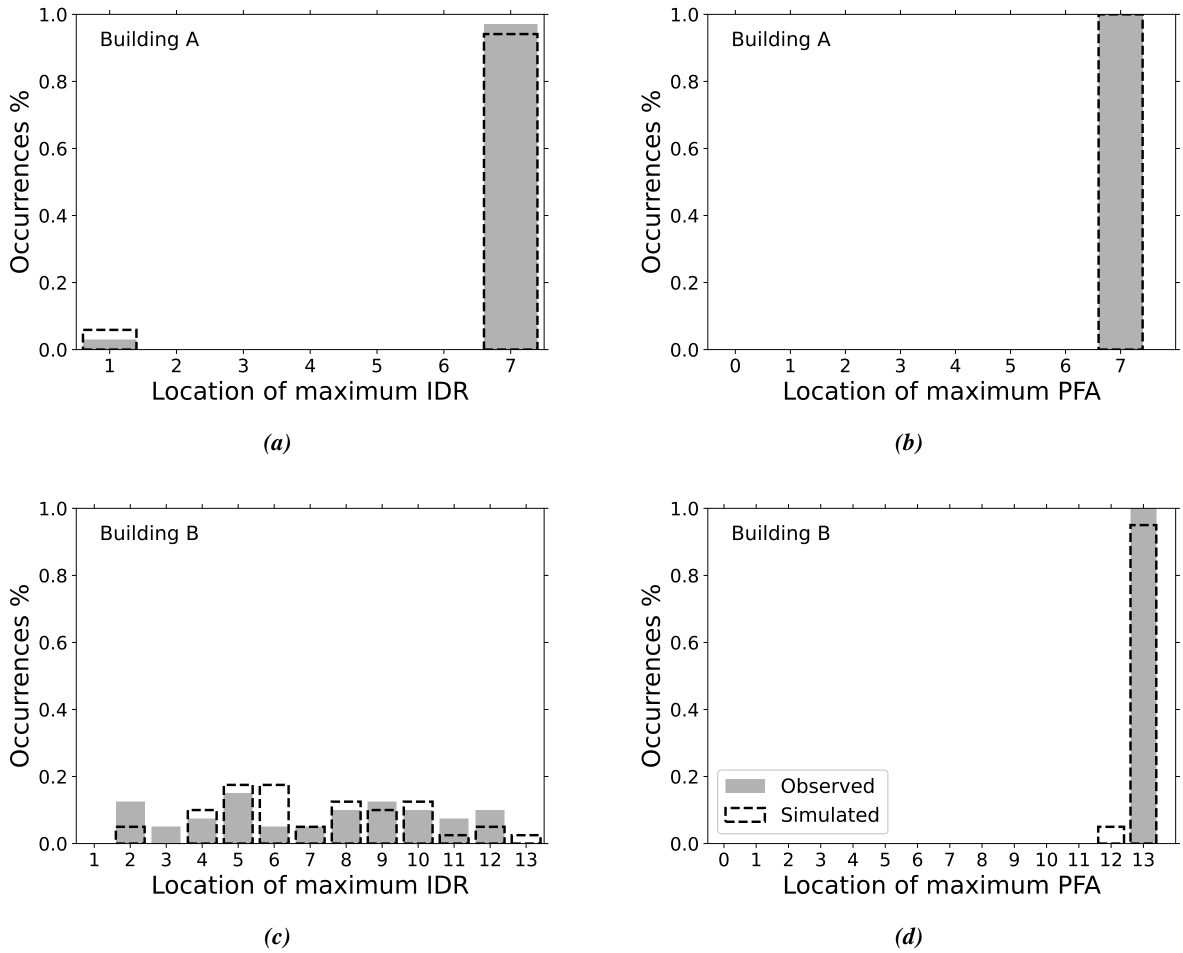

Figure 6: Location of maximum IDR and PFA for (a-b) Building A; and (c-d) Building B in the North-South direction.

case of experiencing nonlinearity (e.g., Building A IDR, Figure 4b). In general, some portion of the differences in the structural response are attributable to the discrepancies between the response spectra at the periods that contribute to the response of interest, as well as differences in other ground motion intensity measures that may affect the response. Since the difference in the structural response is not entirely explained by the difference in the ground motion intensity measures, other complexities in the ground motion characteristics and the structural system (e.g., nonlinearity, torsion) should also be considered when investigating the response of irregular 3D models.

THE EFFECTS OF SAMPLE SIZE ON EDP COMPARISON

In order to ascertain whether the computed differences in the geometric mean of simulated and observed responses are statistically significant, it is necessary to consider the effect of sample size. This effect is scrutinised using the bootstrap technique [47] and hypothesis testing. This is done by drawing random realisations with replacements from the responses of considered ground motions to generate a large ensemble. Also, hypothesis testing is used to check whether there is a systematic difference between two sets of responses. Equality of the geometric mean of responses (from the simulated and observed GMs) is assumed as the null hypothesis. A two-tailed unequal variances *t*-test [48] is performed under the null hypothesis at a significance level of 0.05 following the suggested algorithm by [47]. As previously mentioned, it is assumed that the responses are lognormally distributed. The test statistic under the null hypothesis has a *t*-distribution:

$$t = \frac{\bar{z} - \bar{y}}{\sqrt{\frac{\sigma_z^2}{n} + \frac{\sigma_y^2}{m}}} \tag{1}$$

where $\bar{z}$ and $\bar{y}$ are the sample means, σ_z and σ_y are the sample standard deviations and m, n are the sample sizes.

Since 11 records are suggested as the minimum number of records for response history analysis by the recent versions of building codes [7], 11 records are considered for each realisation of the bootstrapped ensemble (from the set of 40 responses). This determines if there are significant differences, both statistically and practically, when only a subset of 11 ground motions are randomly chosen from the entire set, as specified in the code provisions. The geometric mean of each ensemble is obtained, and then the geometric mean from 5000 realisations of those bootstrapped samples (each with 11 records) is calculated. To assess the statistical significance of the evidence, a p-value is calculated under the null hypothesis (shown in Table 2). A p-value less than 0.05 demonstrates that there is significant evidence for rejecting the null hypothesis (i.e., observed and simulated GMs result in significantly different geometric means for the considered responses). Conversely, there is weak evidence to reject the null hypothesis for the p-values greater than 0.05 (i.e., the geometric mean of observed and simulated GMs responses are similar).

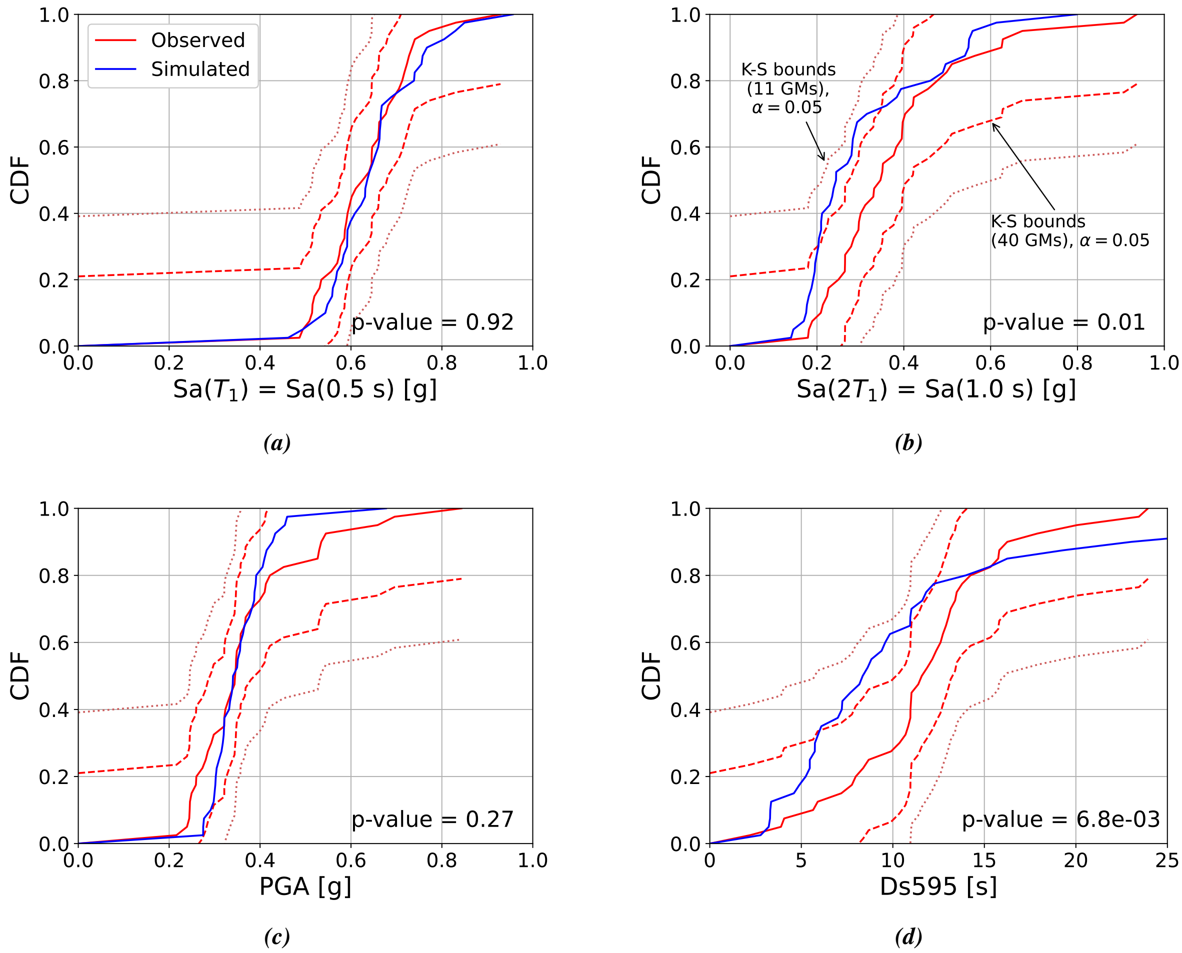

Figure 7: Comparison of the cumulative distribution of a) Sa(T_1); b) Sa($2T_1$); c) PGA, and d) D_{s595} for simulated and observed GMs for Building A. The K-S rejection bounds using the dataset of 40 and 11 GMs for the α=5% significance level are shown in red dashed lines and red dotted lines, respectively.

Figures 12a-b show the comparison between the geometric mean and the 16^{th} and 84^{th} percentiles obtained from all realisations for PFA and peak IDR for Building A. Figure 12b shows a considerable difference in the geometric mean of IDR (with simulated results smaller than the observed) while there is a good agreement in PFA (Figure 12a). As discussed, the difference in the peak IDR is potentially related to the large median spectral acceleration of the observed GMs (Figure 3e) compared to the simulated GMs for periods outside the scaling range ($T>1.3T_1$). As shown in Table 2, the p-values for PFA in all storeys of Building A, except for the fifth and sixth storeys, are greater than the significance level (0.05), which shows the difference for two sets of GMs is not statistically significant in these storeys. The maximum difference between the PFA (Figure 12a) occurs at the sixth storey where the value for observed GMs (0.41g) is 10.2% greater than that for the simulated GMs (0.37g). Nevertheless, the 10% difference in EDPs is likely to be considered acceptable for practical purposes. The maximum difference between IDRs for two groups occurs at the first storey (Figure 12b) where the IDR for observed GMs (0.00349) is 24.5% greater than that for the simulated GMs (0.00263) which is statistically significant (p-value=0.0016). Overall, the calculated p-values for IDR demonstrate that the difference between the two sets of responses is statistically significant for all storeys.

The p-value corresponding to the peak value for a given EDP type across all storeys is also compared in terms of statistical differences (Table 2). The p-values for the maximum PFA and the peak IDR are 0.1792 and 0.0284, respectively, which are quite comparable to the p-values presented for each storey in Table 2 that demonstrate a statistically significant difference for the peak IDR.

Figures 12c-d show the geometric mean and the 16^{th}, and 84^{th} percentiles of all realisation for EDPs for Building B. These figures generally demonstrate a good agreement between the EDPs of two GM sets. The maximum difference between the IDR and PFA of two sets of the observed and simulated responses is quite small (i.e. 1%). Performing hypothesis testing and calculating p-values (presented in Table 3), shows that the differences are not statistically significant for either of the EDPs for Building B (as all values are greater than 0.05). The p-value corresponding to the peak value for a given EDP type across all storeys is also compared in terms of statistical differences (Table 3). The calculated p-values for the maximum PFA and the peak IDR are 0.91 and 0.67, respectively, which indicates that the differences are statistically insignificant for both EDPs.

These findings indicate that simulated ground motions can provide similar results in response history analysis of 3D irregular structural models, as long as the response spectra of the simulations closely match with the observed ground motions. However, it is important to consider a range of periods for amplitude scaling that could potentially impact the structural response (as seen

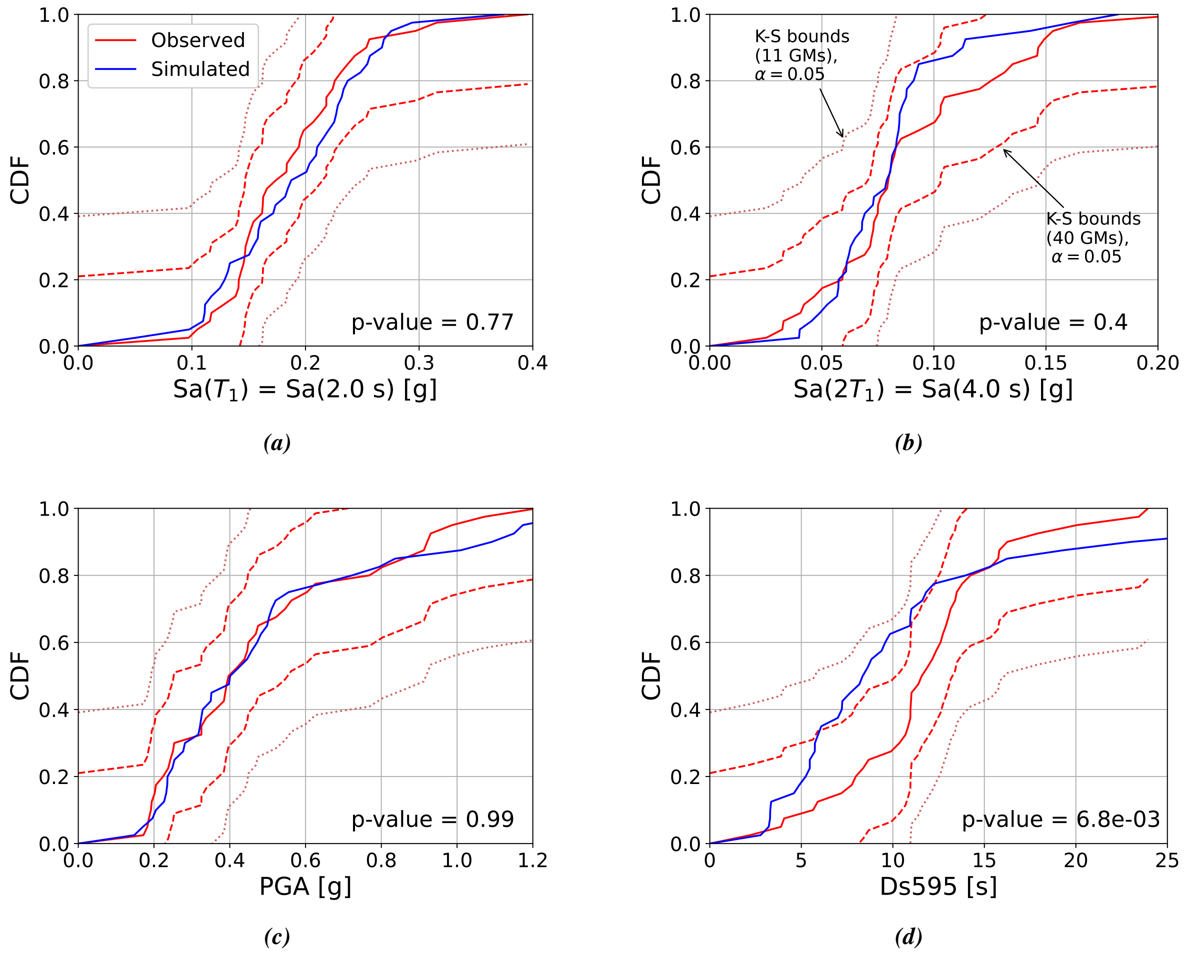

Figure 8: Comparison of the cumulative distribution of a) Sa(T_1); b) Sa($2\mathrm{T}_1$); c) PGA, and d) D_{s595} for simulated and observed GMs for Building B. The K-S rejection bounds using the dataset of 40 and 11 GMs for the α=5% significance level are shown in red dashed lines and red dotted lines, respectively.

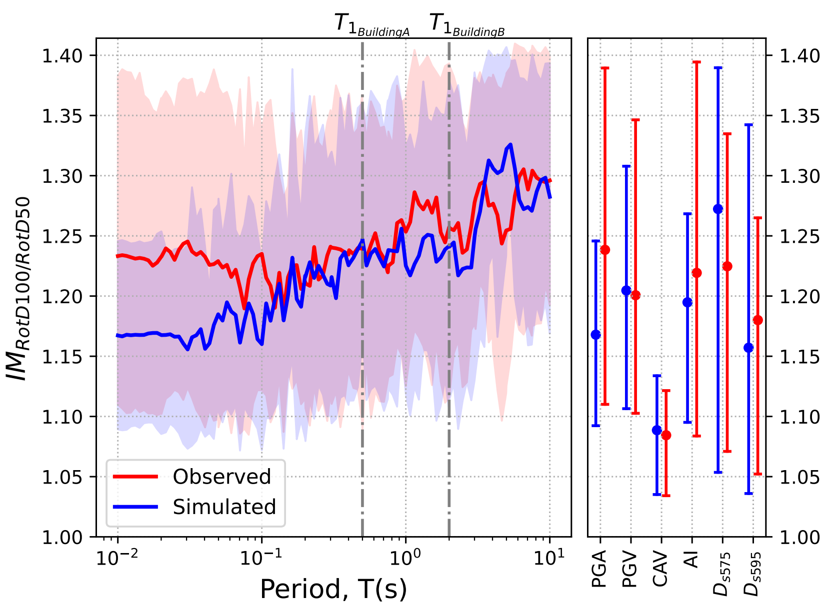

Figure 9: Comparison of geometric mean, and 16^{th}-84^{th} percentiles (shaded region) for the ratio of $RotD100/RotD50$ for the simulated and observed IMs. The grey vertical lines show the fundamental vibration periods.

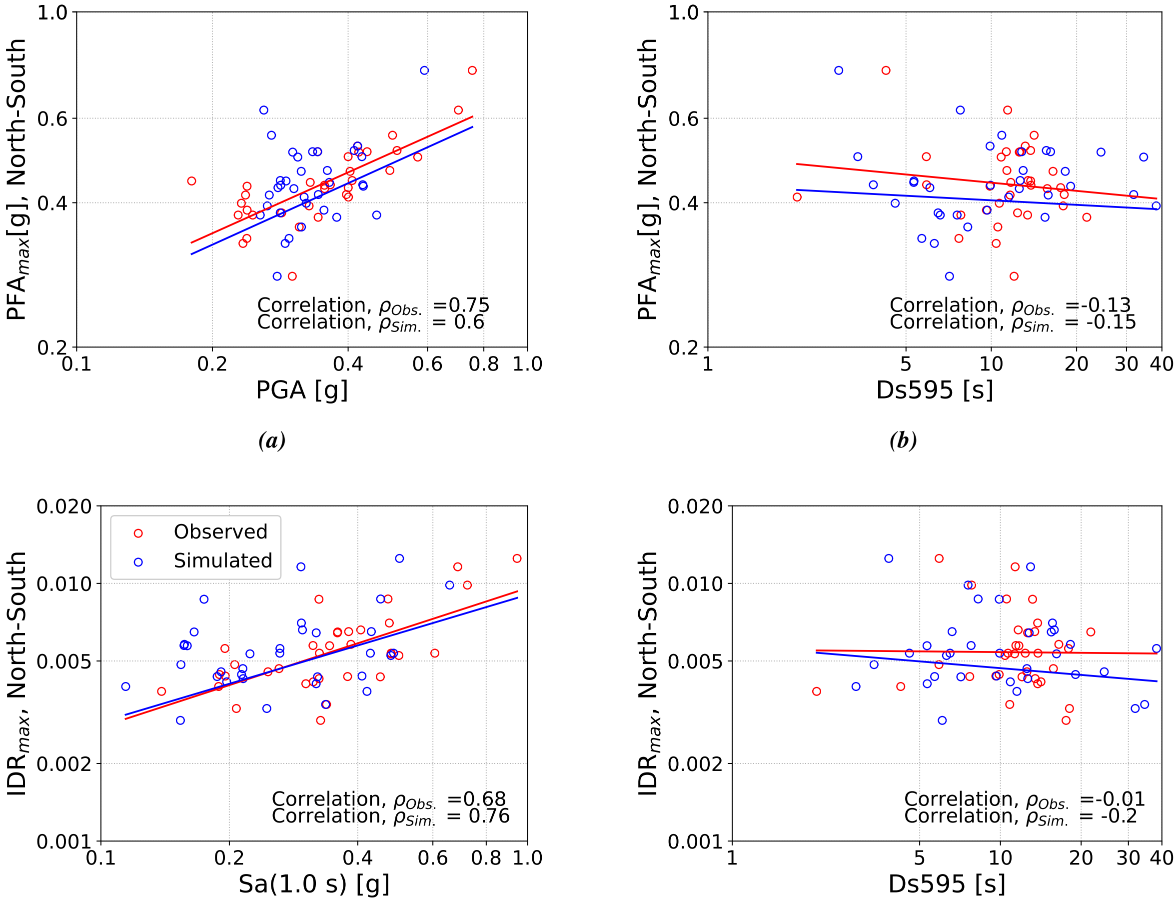

(a) *(b)*

(c) *(d)*

Figure 10: Comparison of maximum PFA across all storeys** (PFA_{max}) **with respect to a) PGA; b)** D_{s595} **and comparison of peak inter-storey drift ratio across all storeys** (IDR_{max}) **with respect to c) Sa(2T_1) and d)** D_{s595} **for simulations and observations in the North-South direction for Building A.

in Building B). Otherwise, any discrepancies in the response spectra may also be reflected in the structural responses (as seen in Building A). The discrepancies in responses that cannot be explained by the differences in the response spectra are attributed to the differences in other ground motions intensity measures and complexities in the structure (e.g., torsion).

CONCLUSIONS

State-of-the-art ground motion (GM) simulation methods provide opportunities to utilise simulated GMs as a supplement or in-place of recorded GMs ensembles for seismic hazard and response history analysis, particularly when there is a paucity of recorded GMs consistent with site-specific hazard in the database. However, validation is required to scrutinise the quality of simulated GMs prior to their utilisation. The validation process, which can be performed at different levels, gives valuable insights for engineers in using simulated GMs as inputs for response history analysis and valuable feedback for GM simulators to improve the simulation methodologies.

In the context of validation for GMs compatible with the design code spectrum, this paper compares responses of two irregular 3D structural models, a seven-storey and a 13-storey building, subjected to 40 recorded and their corresponding simulated GMs of the 22 February 2011 Christchurch earthquake scaled to the NZS1170.5:2004 spectrum. The models represent real buildings, which were designed based on older versions of NZ building codes and physically constructed before the Canterbury earthquake sequences. Attempts are made to investigate the similarities and differences between the PFA and IDR of the systems subjected to observed and simulated GMs when the building code provisions are followed in the analysis and design. Statistical techniques such as bootstrap sampling and hypothesis testing are used to check the comparability of the two datasets.

The results indicate a general agreement between the PFA calculated by the simulated and recorded GMs for the two considered buildings. For the 13-storey building, the hypothesis test results indicate that the differences in IDR are statistically insignificant while they are statistically significant for the seven-storey building (which can potentially be attributed to the greater value of the median of the observed GMs spectrum outside the applied scaling range suggested by the NZS1170.5:2004). The differences, although not likely significant from a practical perspective, could be potentially alleviated by considering a broader period range for matching ground motions to the target spectrum, although this can introduce challenges with the quality of the fit to the target spectrum at other vibration periods with other response metrics might be important. Also, the similarity of torsional responses is investigated by comparing the maximum corner displacement normalised to the centre of mass displacement for simulations and observations. Overall, the findings indicate similar torsional responses between simulated and observed GMs

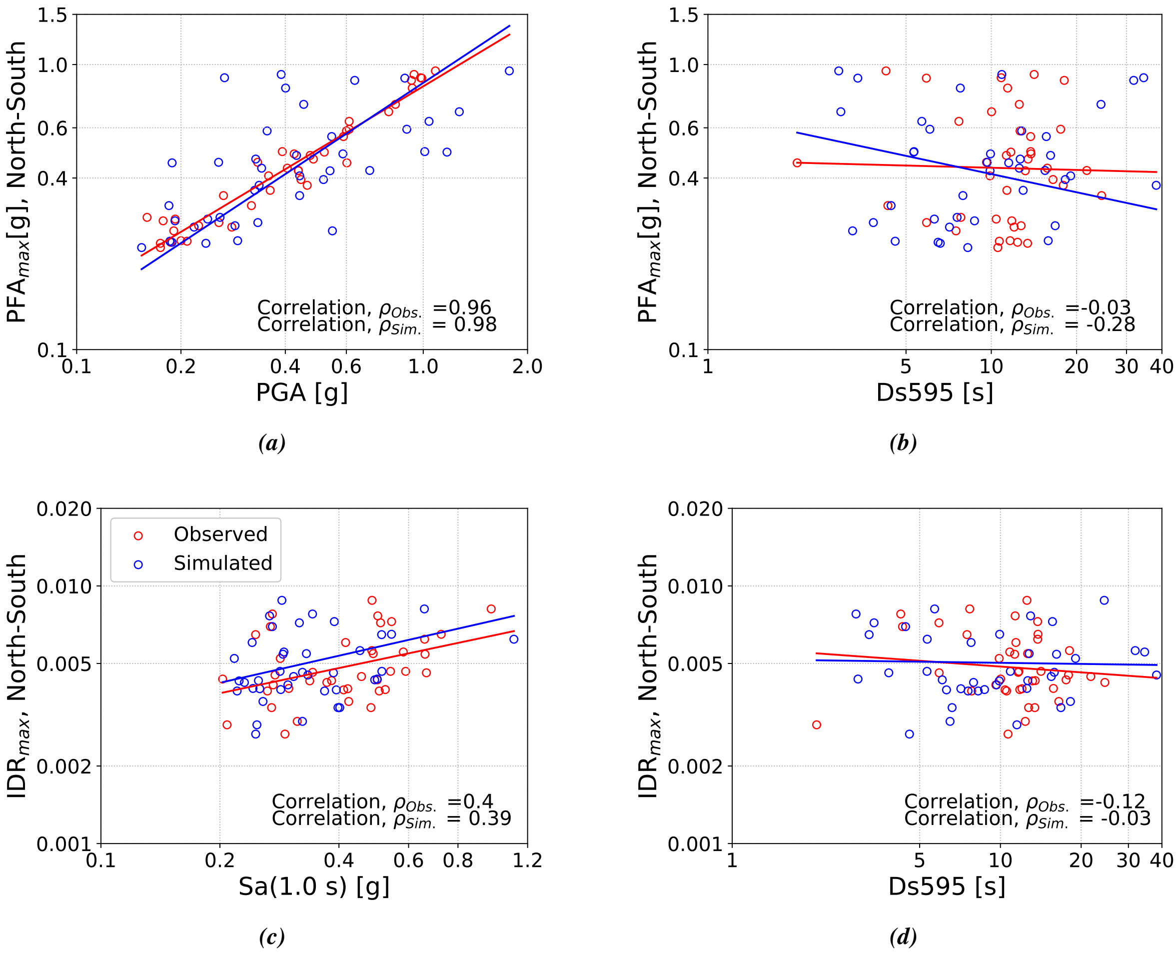

Figure 11: Comparison of maximum PFA across all storeys** (PFA$_{max}$) **with respect to a) PGA; b)** D$_{s595}$ **and comparison of peak inter-storey drift ratio across all storeys** (IDR$_{max}$) **with respect to c) Sa(0.5**T$_1$**) and d)** D$_{s595}$ **for simulations and observations in the North-South direction for Building B.

with a ratio of 0.9 for the storey with the maximum difference. The findings of this paper provide an example, for the specific NZ-based structures and ground motions considered, of the utility of simulated GMs when the code-based approach in response history analysis is followed, and motivate more comprehensive studies to consider a larger array of archetype structures.

ACKNOWLEDGMENTS

The authors would like to thank Holmes Consulting for providing the structural analyses used in this study. Tony Stuart and another anonymous reviewer are acknowledged for provided valuable peer review comments. This work was partially supported by the Natural Hazards Commission, the Marsden Fund, and QuakeCoRE: The NZ Centre for Earthquake Resilience. Ground-motion simulations were performed with high-performance computing resources from the New Zealand eScience Infrastructure (NeSI) [nesi00213] and the Korea Institute of Science and Technology Information (KISTI) [KSC-2023-CRE-0459]. This is QuakeCoRE publication number 1081.

REFERENCES

1 Bradley BA, Pettinga D, Baker JW and Fraser J (2017). “Guidance on the utilization of earthquake-induced ground motion simulations in engineering practice”. *Earthquake Spectra*, **33**(3): 809–835. https://doi.org/10.1193/120216EQS219EP

2 Baker J, Bradley B and Stafford P (2021). *Seismic Hazard and Risk Analysis*. Cambridge University Press, Cambridge, ISBN 978-1-108-42505-6.

3 Tarbali K and Bradley BA (2016). “The effect of causal parameter bounds in PSHA-based ground motion selection”. *Earthquake Engineering & Structural Dynamics*, **45**(9): 1515–1535. https://doi.org/10.1002/eqe.2721

4 Bijelic N, Lin T and Deierlein GG (2018). “Validation of the SCEC Broadband Platform simulations for tall building risk assessments considering spectral shape and duration of the ground motion”. *Earthquake Engineering and Structural Dynamics*, **47**(11): 2233–2251. https://doi.org/10.1002/eqe.3066

5 Baker JW, Rezaeian S, Goulet CA, Luco N and Teng G (2021). “A subset of CyberShake ground-motion time series for response-history analysis”. *Earthquake Spectra*, **37**(2): 1162–1176. https://doi.org/10.1177/8755293020981970

6 Hachem MM, Mathias N, Wang Y, Fajfar P, Tsai K, Ingham J, Oyarzo Vera C and Lee S (2010). “An international comparison of ground motion selection criteria for seismic design”. *Joint IABSE-fib Conference on Codes in Structural Engineering: Developments and Needs for International Practice*, ISBN 9537621065.

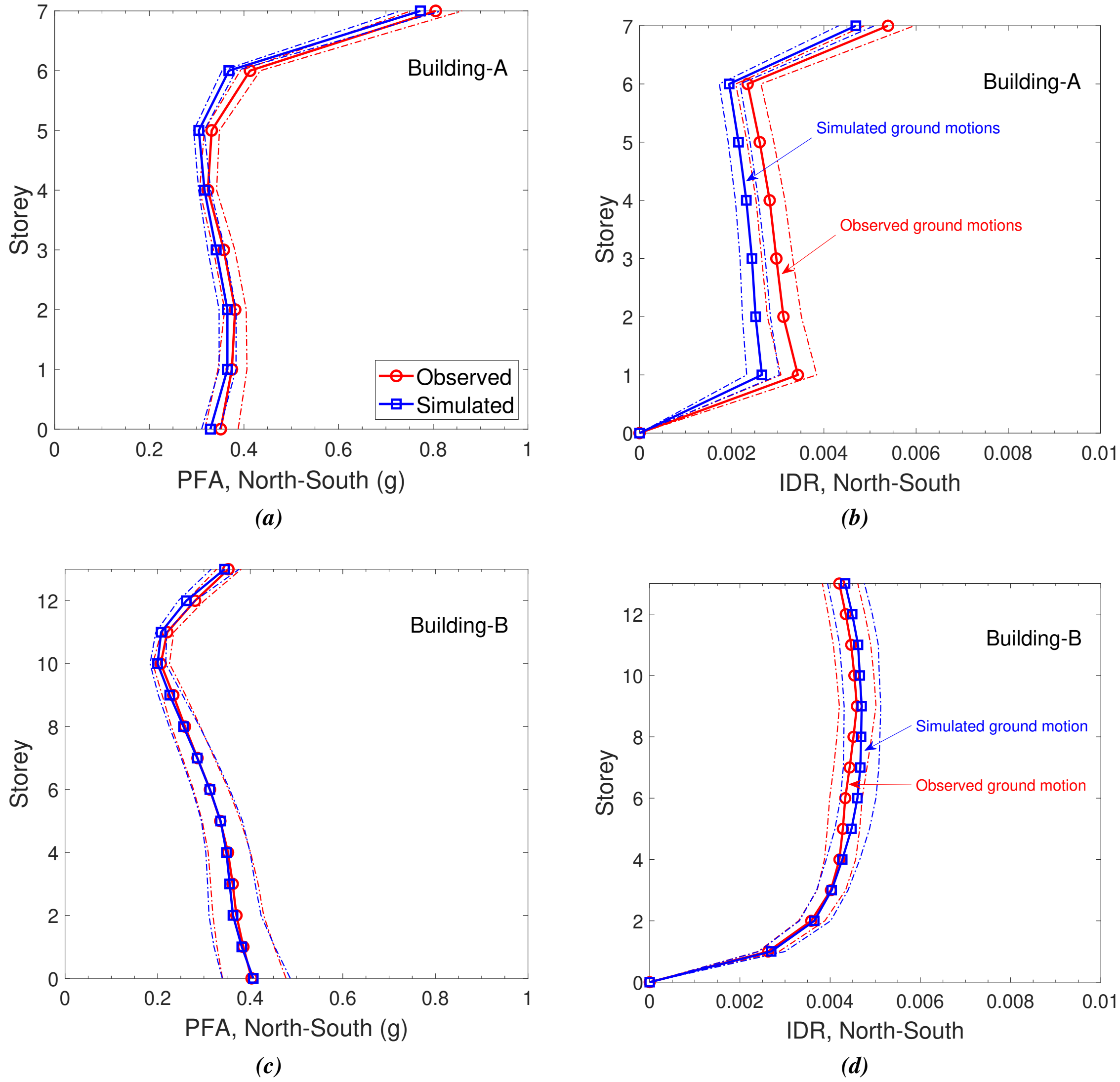

Figure 12: The geometric mean, 16^{th}***, and*** 84^{th} ***percentiles of bootstrapped samples (a) Building A PFA; (b) Building A IDR; (c) Building B PFA; (d) Building B IDR in the North-South direction. Solid lines indicate the geometric mean and dashed lines indicate*** 16^{th}***, and*** 84^{th} ***percentiles.***

7 ASCE-7 (2017). *"Minimum Design Loads and Associated Criteria for Buildings and Other Structures"*. Technical Report ASCE/SEI 7-16, American Society of Civil Engineers, Reston, VA.

8 CEN (2004). *"Eurocode 8 – Design of Structures for Earthquake Resistance, Part 1: General Rules, Seismic Actions and Rules for Buildings"*. Technical Report EN 1998-1, European Committee for Standardization, Brussels.

9 NZS1170.5:2004 (2004). *"Structural Design Actions. Part 5: Earthquake Actions – New Zealand"*. Technical report, Standards New Zealand, Wellington.

10 Lee RL, Bradley BA, Stafford PJ, Graves RW and Rodriguez-Marek A (2022). "Hybrid broadband ground-motion simulation validation of small magnitude active shallow crustal earthquakes in New Zealand". *Earthquake Spectra*, **38**(4): 2548–2579. https://doi.org/10.1177/87552930221109297

11 Lee R, Bradley B, Graves R, Paterson J and Motha J (2021). "Source modelling insights from ground motion simulation validation of moderate magnitude active shallow crustal earthquakes in New Zealand". *2021 New Zealand Society for Earthquake Engineering Annual Technical Conference*, Christchurch, New Zealand, pp. 1–8.

12 Dupuis M, Lee R and Bradley B (2025). "Hybrid broadband ground-motion simulation validation of small-magnitude subduction earthquakes in New Zealand". *Earthquake Spectra*, **41**(5): 4046–4081. https://doi.org/10.1177/87552930251353816

13 Dupuis M (2025). *"Hybrid Broadband Ground-Motion Simulation of Mw3.5–8.7 Subduction Earthquakes in New Zealand"*. Ph.D. Thesis, University of Canterbury, Christchurch, New Zealand. https://doi.org/10.26021/16190

14 Pajaro CA, Bradley B and Lee R (2025). "Validation of hybrid broadband ground-motion simulation for large-magnitude earthquakes in New Zealand". *2025 New Zealand Society for Earthquake Engineering Annual Technical Conference*, Auckland, New Zealand, p. 9.

Table 2: P-values for Building A responses at each storey in the North-South direction[1].

EDP/Storey	0	1	2	3	4	5	6	7	Max EDP*
PFA	0.28	0.52	0.176	0.137	0.324	**0.0072**	**0.0076**	0.184	0.1792
IDR	—	**0.0016**	**0.0052**	**0.0052**	**0.0044**	**0.0076**	**0.014**	**0.0236**	**0.0284**

[1] *Statistically significant values at the 0.05 level are denoted in bold.*

Table 3: P-values for Building B responses at each storey in the North-South direction.

EDP/Storey	0	1	2	3	4	5	6	7	8	9	10	11	12	13	Max EDP*
PFA	0.89	0.91	0.72	0.73	0.83	0.98	0.99	0.97	0.87	0.59	0.52	0.1	0.09	0.60	0.91
IDR	—	0.74	0.78	0.96	0.82	0.43	0.27	0.33	0.47	0.66	0.59	0.49	0.52	0.58	0.67

**Maximum response across all storeys.*

15 Bazzurro P, Sjoberg B and Luco N (2004). *"Post-Elastic Response of Structures to Synthetic Ground Motions"*. Technical report, Pacific Earthquake Engineering Research (PEER) Center Lifelines Program Project, Berkeley, CA, 65–112.

16 Iervolino I, De Luca F and Cosenza E (2010). "Spectral shape-based assessment of SDOF nonlinear response to real, adjusted and artificial accelerograms". *Engineering Structures*, **32**(9): 2776–2792. https://doi.org/10.1016/j.engstruct.2010.04.047

17 Atkinson GM and Goda K (2010). "Inelastic seismic demand of real versus simulated ground-motion records for Cascadia subduction earthquakes". *Bulletin of the Seismological Society of America*, **100**(1): 102–115. https://doi.org/10.1785/0120090023

18 Galasso C, Zareian F, Iervolino I and Graves R (2012). "Validation of ground-motion simulations for historical events using SDoF systems". *Bulletin of the Seismological Society of America*, **102**(6): 2727–2740. https://doi.org/10.1785/0120120018

19 Jayaram N and Shome N (2012). "A statistical analysis of the response of tall buildings to recorded and simulated ground motions". *15th World Conference on Earthquake Engineering*, Lisbon, Portugal, pp. 1–10.

20 Galasso C, Zhong P, Zareian F, Iervolino I and Graves RW (2013). "Validation of ground-motion simulations for historical events using MDoF systems". *Earthquake Engineering & Structural Dynamics*, **42**(9): 1395–1412. https://doi.org/10.1002/eqe.2278

21 Bijelic N, Lin T and Deierlein G (2014). "Seismic response of a tall building to recorded and simulated ground motions". *Tenth U.S. National Conference on Earthquake Engineering, Frontiers of Earthquake Engineering*, Anchorage, AK.

22 Burks LS, Zimmerman RB and Baker JW (2015). "Evaluation of hybrid broadband ground motion simulations for response history analysis and design". *Earthquake Spectra*, **31**(3): 1691–1710. https://doi.org/10.1193/091113EQS248M

23 Galasso C, Kaviani P, Tsioulou A and Zareian F (2020). "Validation of ground motion simulations for historical events using skewed bridges". *Journal of Earthquake Engineering*, **24**(10): 1652–1674. https://doi.org/10.1080/13632469.2018.1483277

24 SESOC (2025). *"Nonlinear Response History Analysis Design Guide"*. Technical report, Structural Engineering Society New Zealand, Wellington, New Zealand.

25 Standards New Zealand (2025). *"Technical Specification: Structural Design Actions. Part 5: Earthquake Actions – New Zealand"*. Technical Report TS 1170.5:2025, Standards New Zealand, Wellington.

26 NZS4203:1976 (1976). *"Code of Practice for General Structural Design and Design Loadings for Buildings"*. Technical report, Standards New Zealand, Wellington.

27 NZS3101:1982 (1982). *"Code of Practice for Design of Concrete Structures"*. Technical report, Standards New Zealand, Wellington.

28 CERC (2012). *"The Performance of Christchurch CBD Buildings"*. Technical report, Canterbury Earthquakes Royal Commission, Christchurch, New Zealand.

29 Mondkar D and Powell G (1979). *"ANSR-II: Analysis of Nonlinear Structural Response - User Manual"*. Technical Report UCB/EERC-79/17, Earthquake Engineering Research Center.

30 FEMA (2000). *"Prestandard and Commentary for the Seismic Rehabilitation of Buildings"*. Technical Report FEMA 356, Federal Emergency Management Agency, Washington, DC.

31 Razafindrakoto HN, Bradley BA and Graves RW (2018). "Broadband ground-motion simulation of the 2011 Mw 6.2 Christchurch, New Zealand, earthquake". *Bulletin of the Seismological Society of America*, **108**(4): 2130–2147. https://doi.org/10.1785/0120170388

32 Graves RW and Pitarka A (2010). "Broadband ground-motion simulation using a hybrid approach". *Bulletin of the Seismological Society of America*, **100**(5A): 2095–2123. https://doi.org/10.1785/0120100057

33 Graves RW and Pitarka A (2015). "Refinements to the Graves and Pitarka (2010) broadband ground-motion simulation method". *Seismological Research Letters*, **86**(1): 75–80. https://doi.org/10.1785/0220140101

34 Shome N (1999). *"Probabilistic Seismic Demand Analysis of Nonlinear Structures"*. Ph.D. Thesis, Stanford University, Stanford, CA.

35 Aslani H and Miranda E (2003). *"Probabilistic Response Assessment for Building-Specific Loss Estimation"*. Technical Report PEER 2003/03, Pacific Earthquake Engineering Research Center, University of California, Berkeley, CA.

36 Fajfar P, Marusic D and Perus I (2005). "Torsional effects in the pushover-based seismic analysis of buildings". *Journal of Earthquake Engineering*, **9**(06): 831–854. https://doi.org/10.1080/13632460509350568

37 Marusic D and Fajfar P (2005). “On the inelastic seismic response of asymmetric buildings under bi-axial excitation”. *Earthquake Engineering and Structural Dynamics*, **34**(8): 943–963. https://doi.org/10.1002/eqe.463

38 Erduran E and Ryan KL (2011). “Effects of torsion on the behavior of peripheral steel-braced frame systems”. *Earthquake Engineering and Structural Dynamics*, **40**(5): 491–507. https://doi.org/10.1002/eqe.1032

39 Ibarra LF and Krawinkler H (2005). *“Global Collapse of Frame Structures under Seismic Excitations”*. Technical Report PEER 2005/06, Pacific Earthquake Engineering Research Center, University of California, Berkeley, CA.

40 Krawinkler H, Zareian F, Medina RA and Ibarra LF (2006). “Decision support for conceptual performance-based design”. *Earthquake Engineering & Structural Dynamics*, **35**(1): 115–133. https://doi.org/10.1002/eqe.536

41 Zareian F and Krawinkler H (2007). “Assessment of probability of collapse and design for collapse safety”. *Earthquake Engineering & Structural Dynamics*, **36**(13): 1901–1914. https://doi.org/10.1002/eqe.702

42 Ang A and Tang W (1975). *Probability Concepts in Engineering Planning and Design, Volume I, Basic Principles*. Wiley, New York.

43 Boore DM, Watson-Lamprey J and Abrahamson NA (2006). “Orientation-independent measures of ground motion”. *Bulletin of the Seismological Society of America*, **96**(4A): 1502–1511. https://doi.org/10.1785/0120050209

44 Boore DM (2010). “Orientation-independent, nongeometric-mean measures of seismic intensity from two horizontal components of motion”. *Bulletin of the Seismological Society of America*, **100**(4): 1830–1835. https://doi.org/10.1785/0120090400

45 Shahi SK and Baker JW (2014). “NGA-West2 models for ground motion directionality”. *Earthquake Spectra*, **30**(3): 1285–1300. https://doi.org/10.1193/040913EQS097M

46 Stewart JP, Abrahamson NA, Atkinson GM, Baker JW, Boore DM, Bozorgnia Y, Campbell KW, Comartin CD, Idriss I and Lew M (2011). “Representation of bidirectional ground motions for design spectra in building codes”. *Earthquake Spectra*, **27**(3): 927–937. https://doi.org/10.1193/1.3608001

47 Efron B and Tibshirani RJ (1994). *An introduction to the bootstrap*. CRC press, ISBN 0412042312.

48 Welch BL (1938). “The significance of the difference between two means when the population variances are unequal”. *Biometrika*, **29**(3/4): 350–362. https://doi.org/10.2307/2332010

APPENDIX

Table A.1 shows the station name, geographic location, and V_{s30} for the considered stations.

Figure A.1-Figure A.12 provide supplementary figures not provided in the main text. All responses are reported at the centre of mass (CM).

Table A.1: Station name, geographic location and V_{s30} ***for the selected stations.***

Site	**Longitude** (°)	**Latitude** (°)	V_{s30}**(m/s)**
ADCS	171.7476	-43.9024	300
ASHS	172.5959	-43.2744	300
CACS	172.53	-43.4832	435
CBGS	172.6199	-43.5293	197
CCCC	172.6474	-43.5381	182
CHHC	172.6275	-43.5359	196
CMHS	172.6242	-43.5656	213
CSHS	171.7236	-43.2265	800
CSTC	172.3813	-43.3123	350
D06C	172.6142	-43.5402	200
D09C	172.6325	-43.5339	200
DFHS	172.1022	-43.4897	400
DORC	172.0938	-43.8968	300
DSLC	172.1979	-43.6675	350
HORC	171.9599	-43.5396	350
HPSC	172.7022	-43.5016	196
HVSC	172.7094	-43.5798	350
KOWC	171.8549	-43.3215	350
KPOC	172.6638	-43.3765	257
LPCC	172.7248	-43.6078	792
LPOC	172.712	-43.609	200
MQZ	172.6538	-43.7061	800
NNBS	172.718	-43.4954	204
OXZ	172.0383	-43.3259	350
PPHS	172.6069	-43.4928	180
PRPC	172.6828	-43.5258	196
REHS	172.6351	-43.5219	155
RHSC	172.5644	-43.5362	286
RKAC	172.0231	-43.7515	300
ROLC	172.3811	-43.5928	350
SBRC	172.2524	-43.8087	200
SHFC	172.0258	-43.3912	350
SHLC	172.6634	-43.5053	201
SLRC	172.3175	-43.6751	350
SMTC	172.6139	-43.4675	219
SPFS	171.9289	-43.338	450
SWNC	172.4954	-43.3694	400
TPLC	172.472	-43.55	350
WSFC	171.611	-43.8373	350

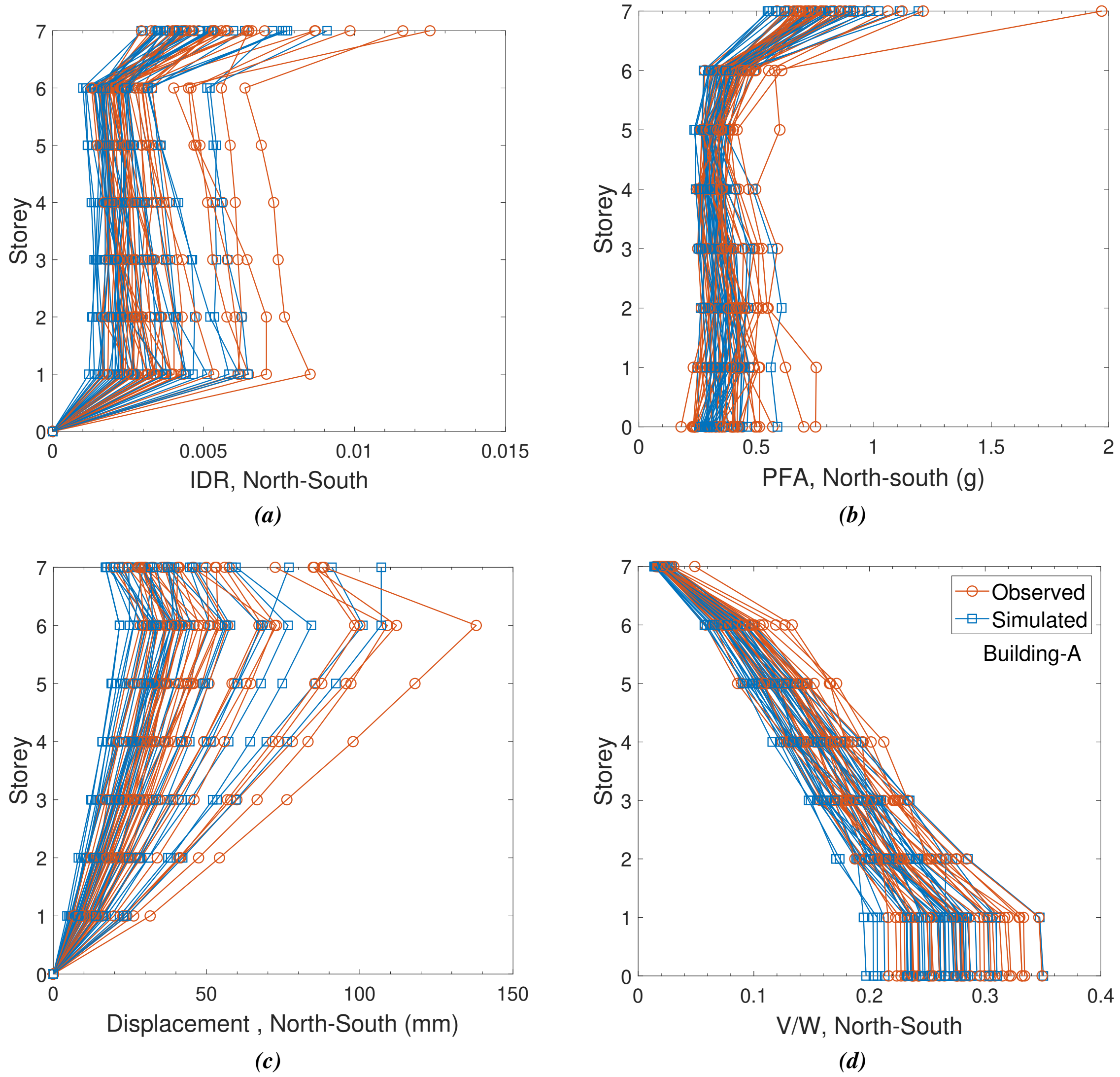

Figure A.1: The absolute value of responses for the considered ground motions (a) inter-storey drift ratio (IDR); (b) peak floor acceleration (PFA); (c) displacement; (d) normalised storey shear for Building A in the North-South direction.

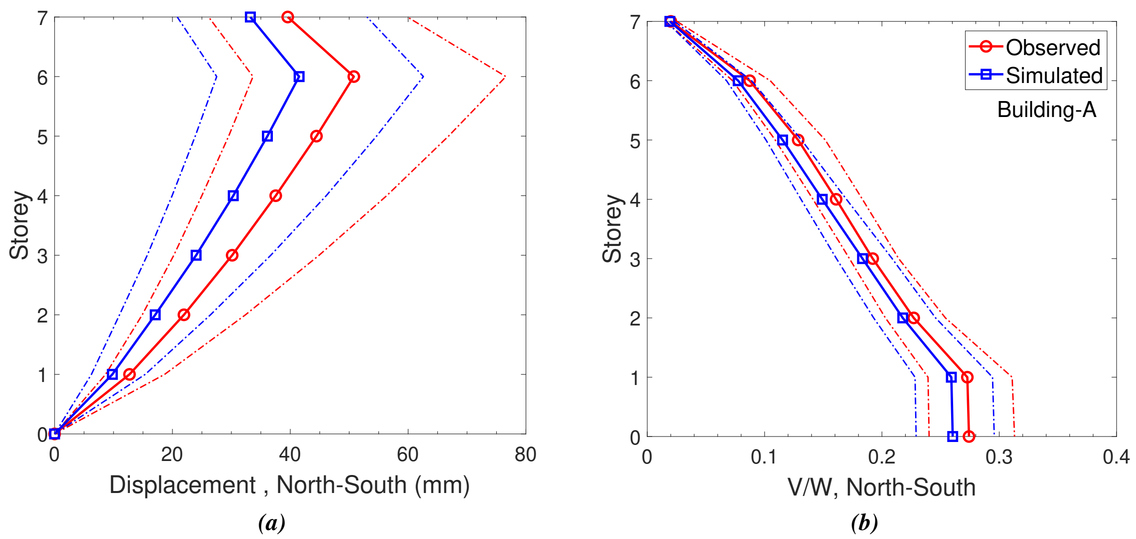

Figure A.2: The geometric mean, and percentiles of simulated and observed responses at the centre of mass for (a) displacement; (b) normalised storey shear for Building A in the North-South direction.

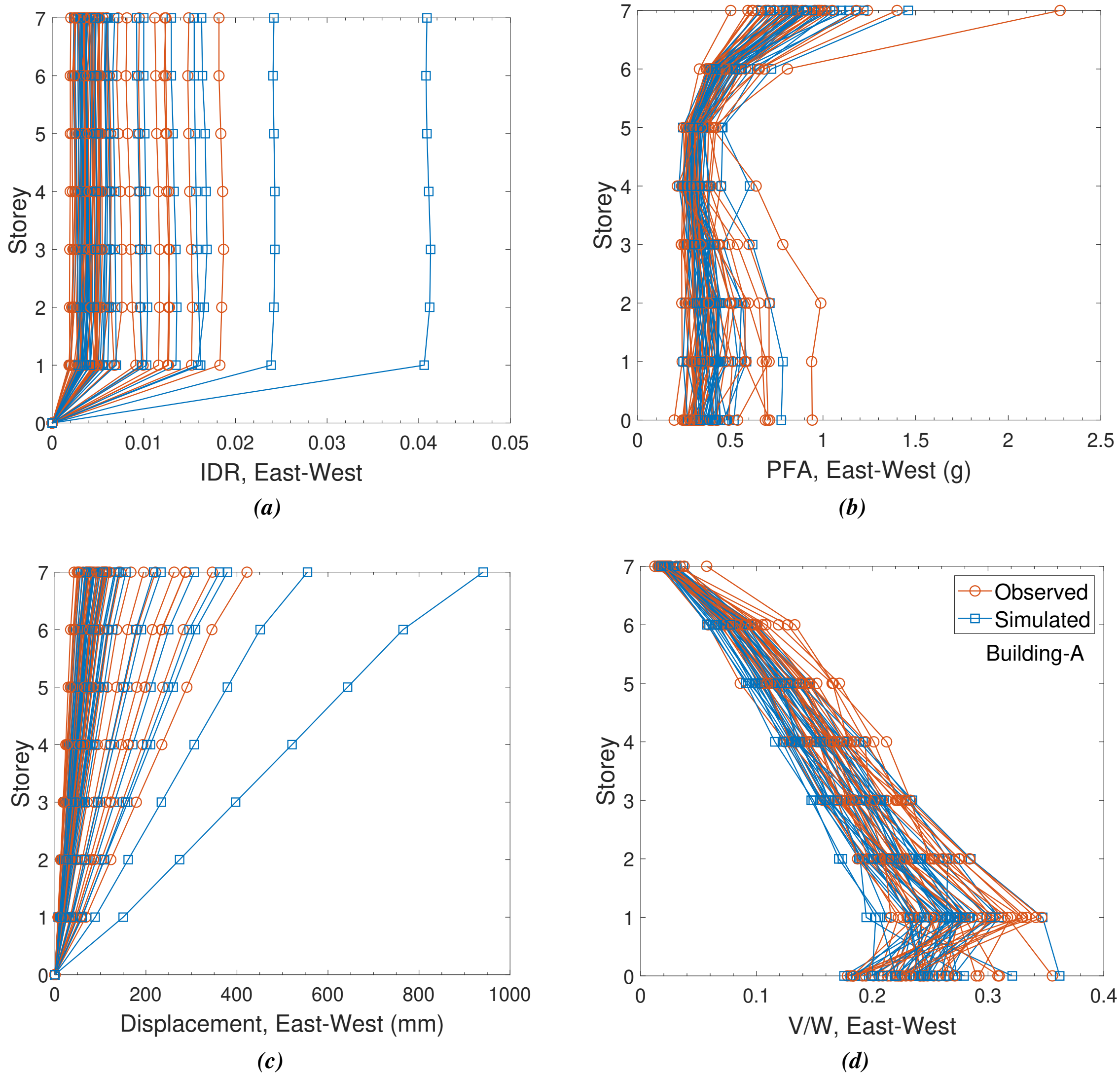

Figure A.3: The absolute value of responses for the considered ground motions (a) inter-storey drift ratio (IDR); (b) peak floor acceleration (PFA); (c) displacement; (d) normalised storey shear for Building A in the East-West direction.

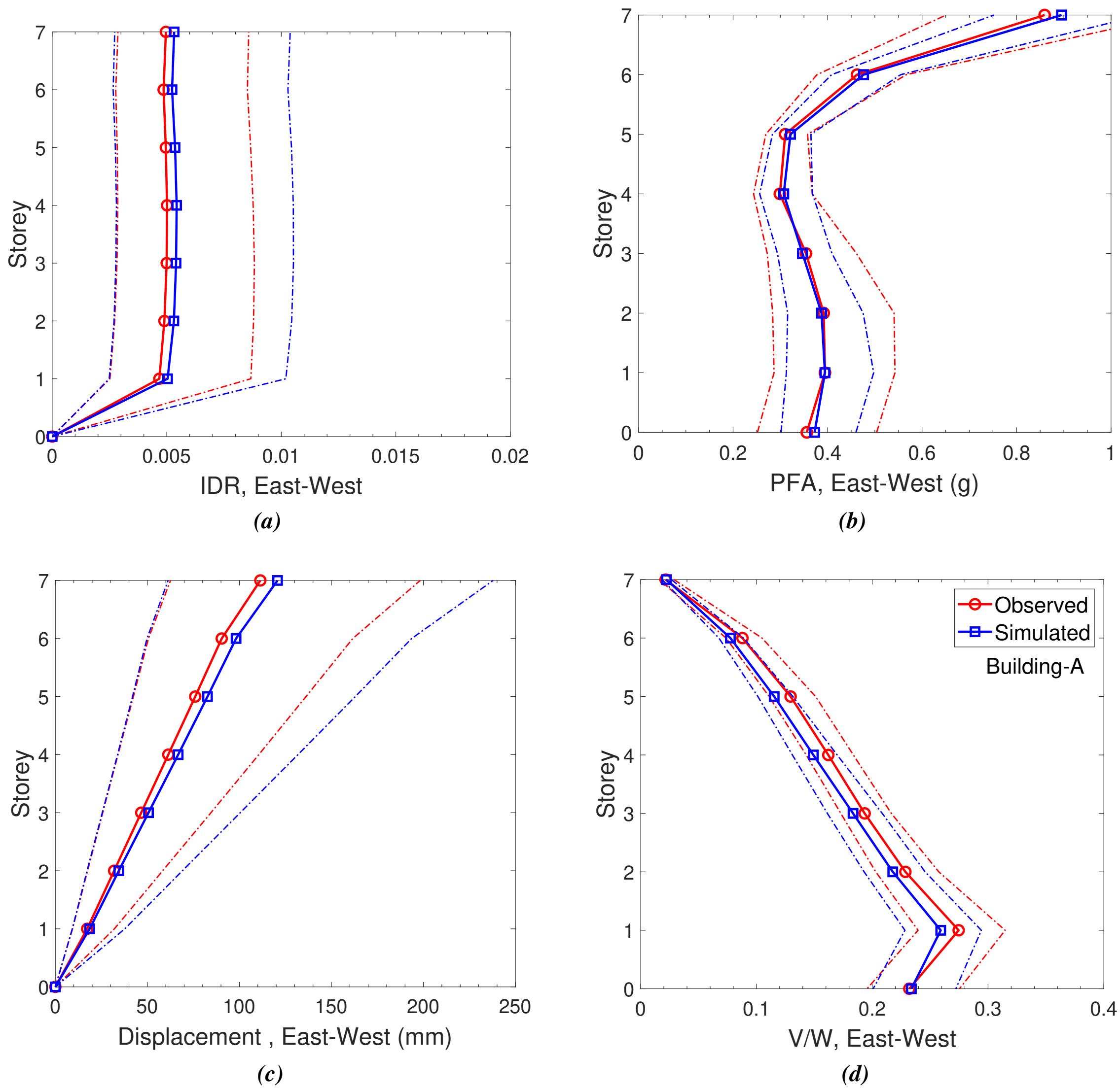

Figure A.4: The geometric mean, and percentiles of simulated and observed responses at the centre of mass for (a) displacement; (b) normalised storey shear for Building A in the East-West direction.

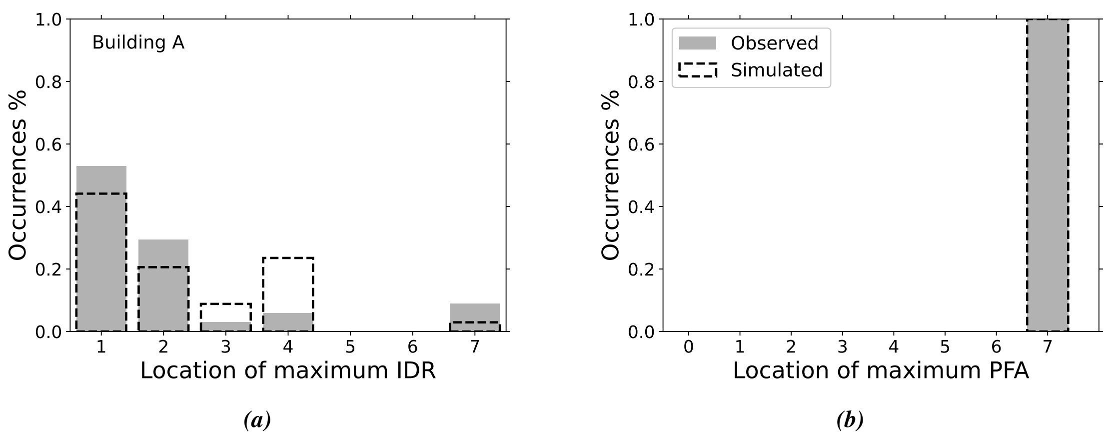

Figure A.5: Location of maximum (a) inter-storey drift ratio (IDR); and (b) peak floor acceleration (PFA) for Building A in the East-West direction.

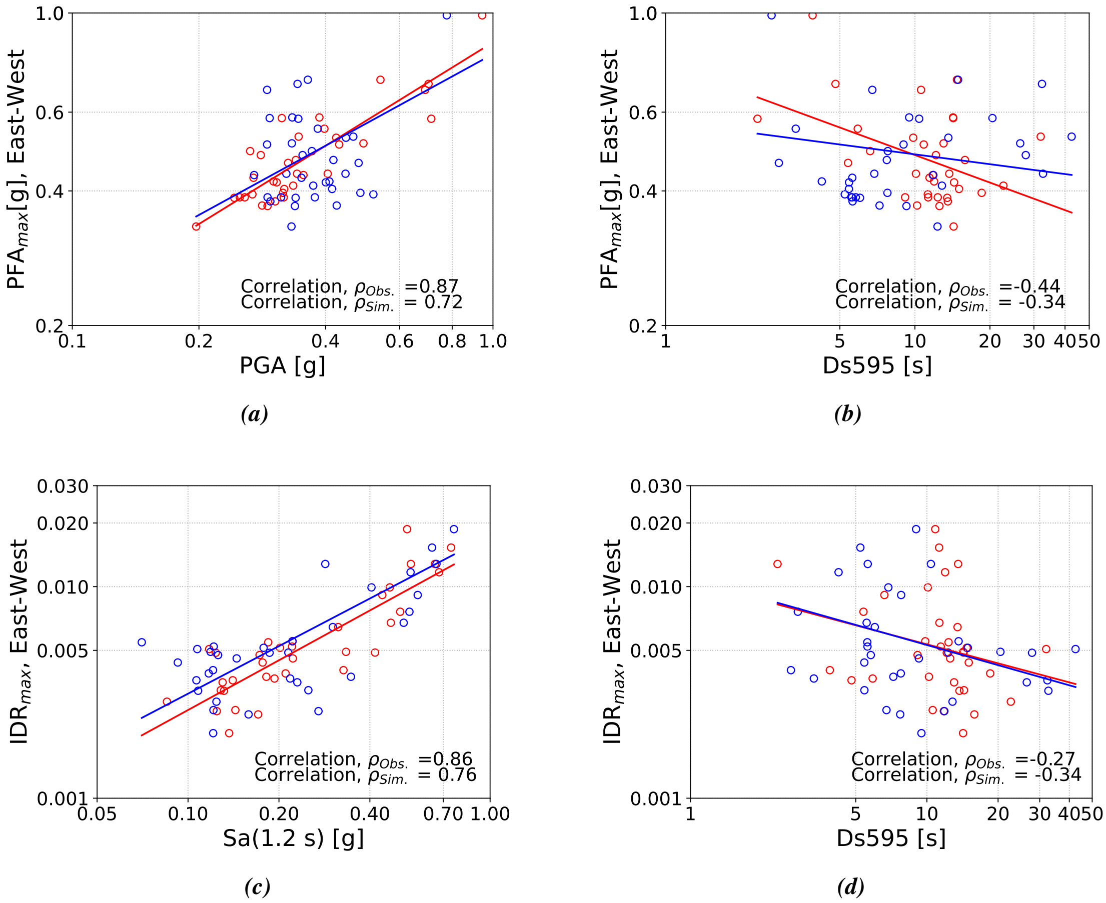

Figure A.6: Comparison of maximum peak floor acceleration across all storeys (PFA$_{max}$) with respect to a) PGA; b) D$_{s595}$ and comparison of peak inter-storey drift ratio across all storeys (IDR$_{max}$) with respect to c) Sa(2.5T$_1$) and d) D$_{s595}$ for simulations and observations in the East-West direction for Building A.

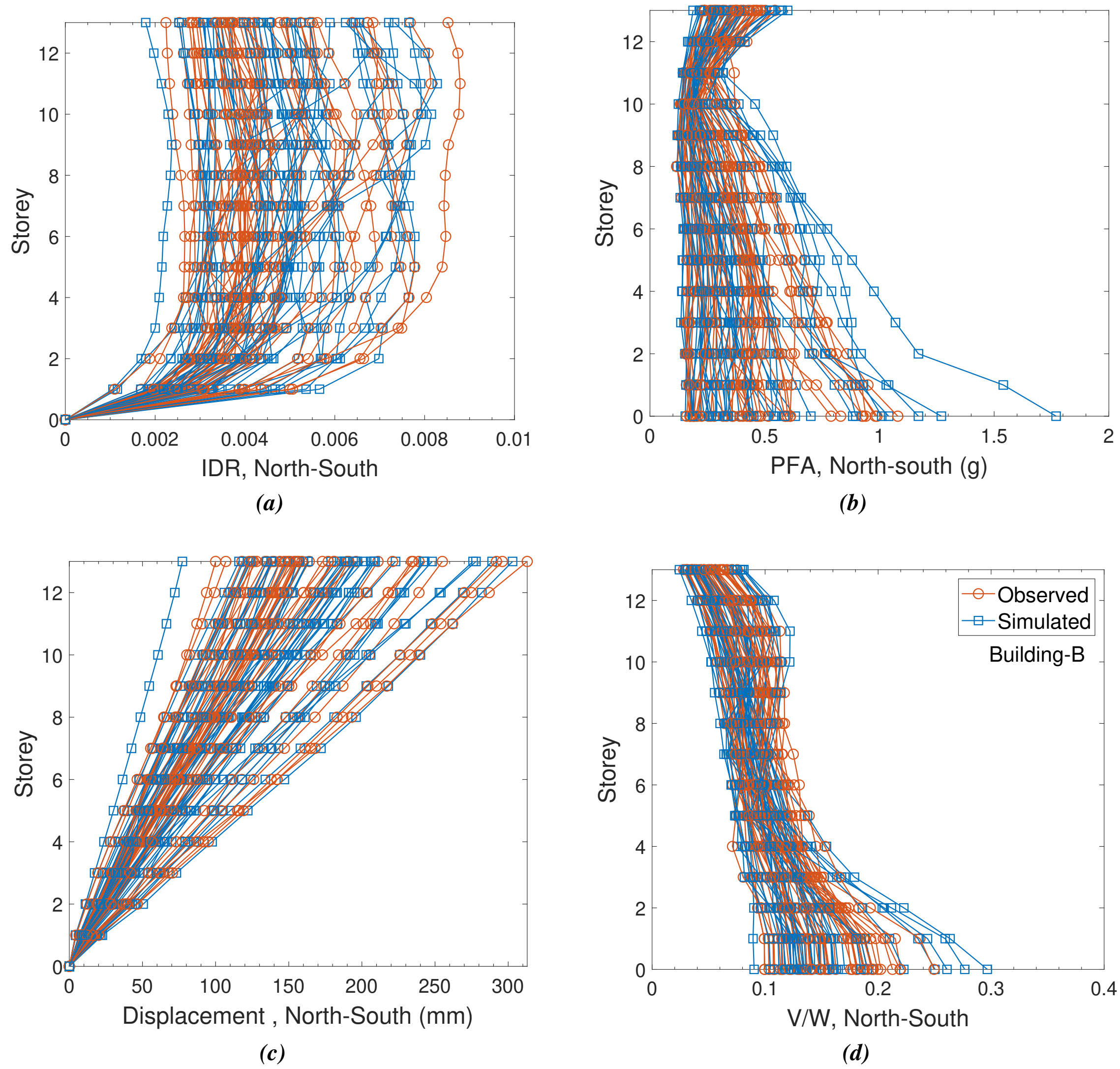

Figure A.7: The absolute value of responses for the considered ground motions (a) inter-storey drift ratio (IDR); (b) peak floor acceleration (PFA); (c) displacement; (d) normalised storey shear for Building B in the North-South direction.

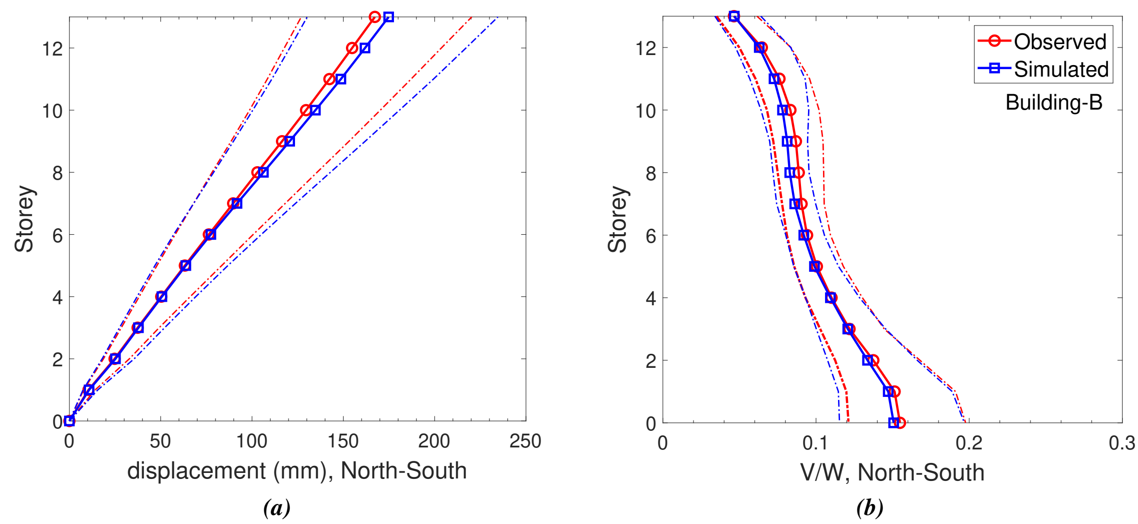

Figure A.8: The geometric mean, and percentiles of simulated and observed responses at the centre of mass for (a) displacement; (b) normalised storey shear for Building B in the North-South direction.

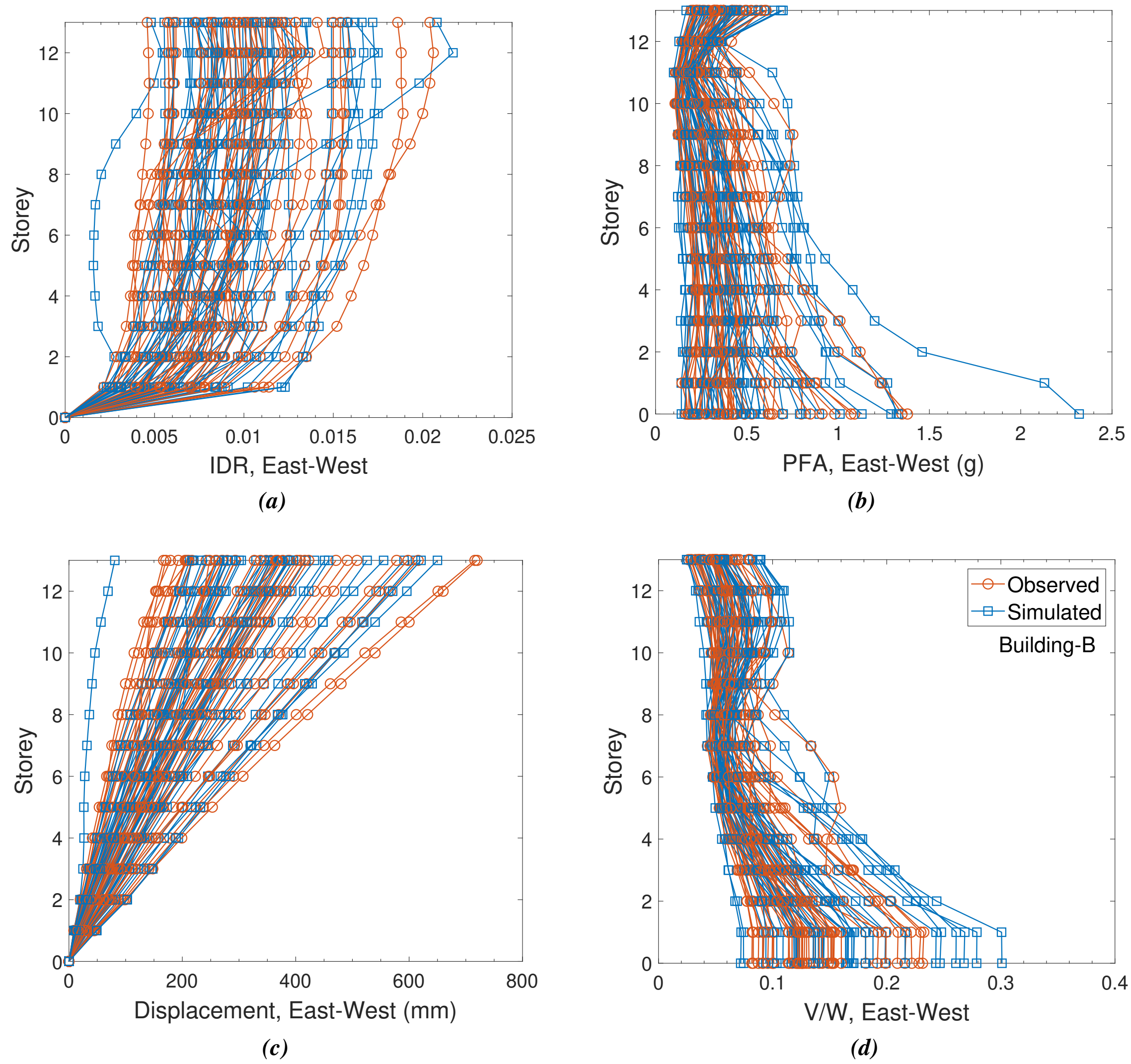

Figure A.9: The absolute value of responses for the considered ground motions (a) inter-storey drift ratio (IDR); (b) peak floor acceleration (PFA); (c) displacement; (d) normalised storey shear for Building B in the East-West direction.

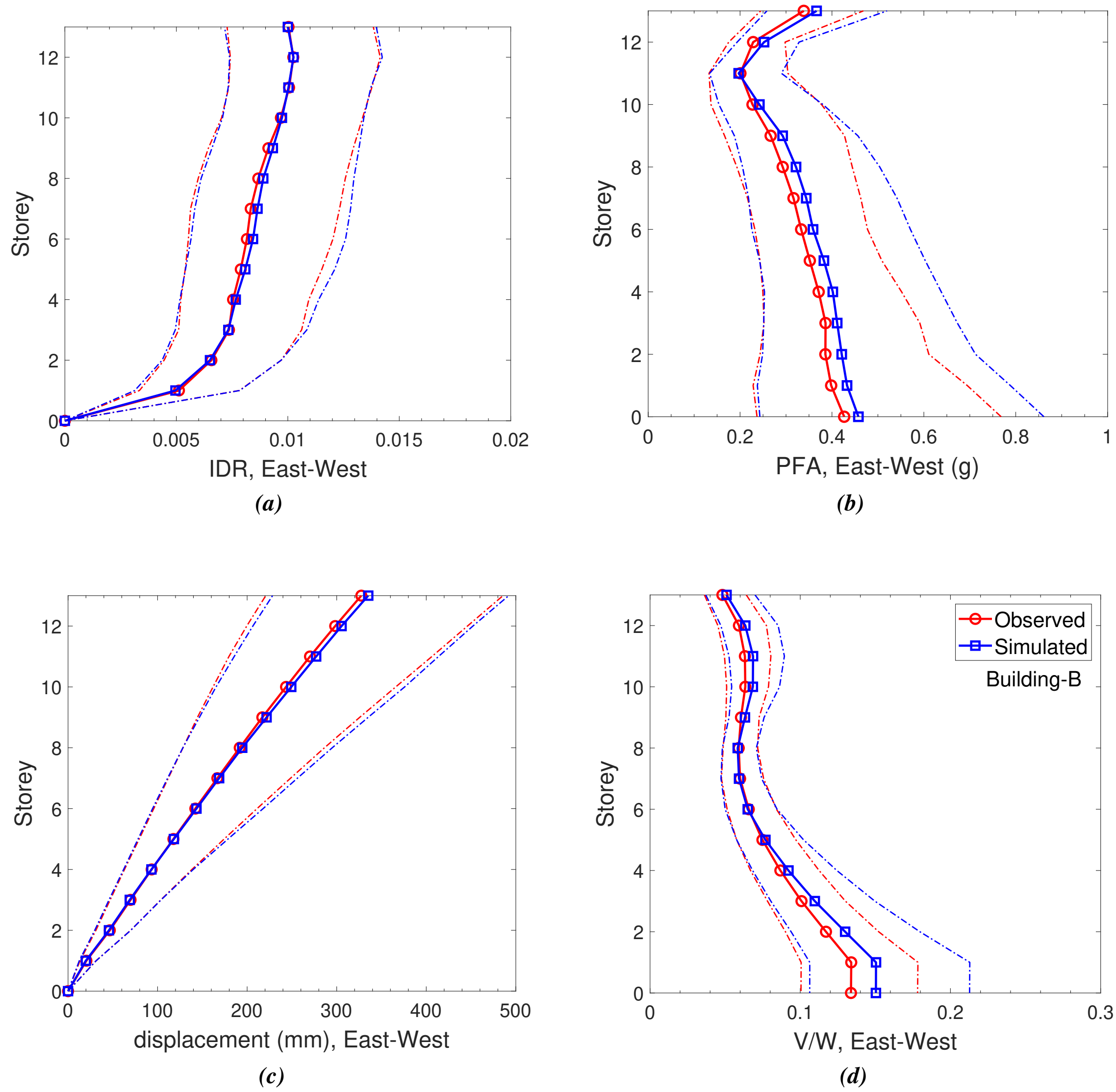

Figure A.10: The geometric mean, and percentiles of simulated and observed responses at the centre of mass for (a) displacement; (b) normalised storey shear for Building B in the East-West direction.

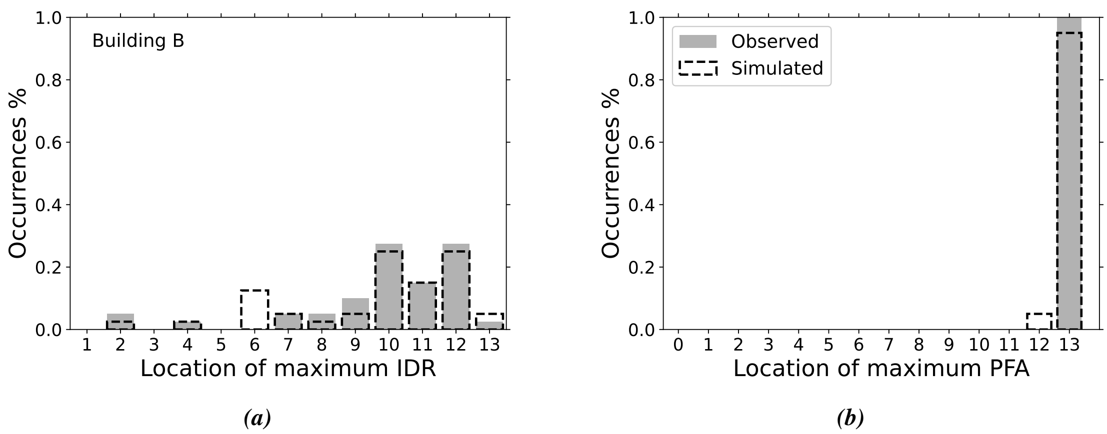

Figure A.11: Location of maximum (a) IDR; and (b) PFA for Building B in the East-West direction.

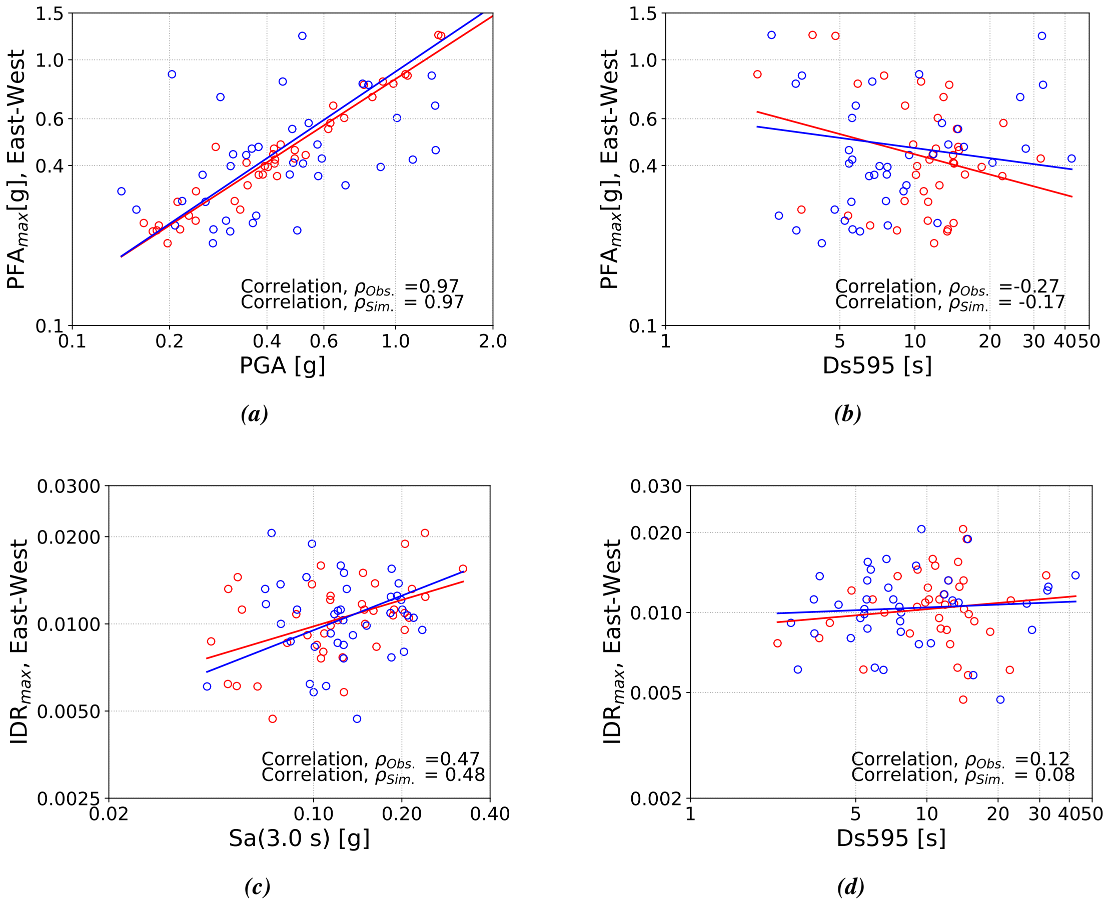

Figure A.12: Comparison of maximum peak floor acceleration across all storeys (PFA$_{max}$) ***with respect to a) PGA; b)*** D$_{s595}$ ***and comparison of peak inter-storey drift ratio across all storeys*** (IDR$_{max}$) ***with respect to c) Sa(1.5***T$_1$***) and d)*** D$_{s595}$ ***for simulations and observations in the East-West direction for Building B.***